Published for SISSA by Springer

Received: December 13, 2022
Accepted: March 13, 2023
Published: March 27, 2023

String-scale gauge coupling relations in the supersymmetric Pati-Salam models from intersecting D6-branes

Tianjun Li,[a,b,c] **Rui Sun**[d] **and Lina Wu**[1,a]

[a] *School of Sciences, Xi'an Technological University, Xi'an 710021, P.R. China*
[b] *CAS Key Laboratory of Theoretical Physics, Institute of Theoretical Physics, Chinese Academy of Sciences, Beijing 100190, P.R. China*
[c] *School of Physical Sciences, University of Chinese Academy of Sciences, No.19A Yuquan Road, Beijing 100049, P.R. China*
[d] *Korea Institute for Advanced Study, 85 Hoegiro, Dongdaemun-Gu, Seoul 02455, Korea*

E-mail: tli@itp.ac.cn, sunrui@kias.re.kr, wulina@xatu.edu.cn

Abstract: We have constructed all the three-family $\mathcal{N} = 1$ supersymmetric Pati-Salam models from intersecting D6-branes, and obtained 33 independent models in total. But how to realize the string-scale gauge coupling relations in these models is a big challenge. We first discuss how to decouple the exotic particles in these models. In addition, we consider the adjoint chiral mulitplets for $SU(4)_C$ and $SU(2)_L$ gauge symmetries, the Standard Model (SM) vector-like particles from D6-brane intersections, as well as the vector-like particles from the $\mathcal{N} = 2$ subsector. We show that the gauge coupling relations at string scale can be achieved via two-loop renormalization group equation running for all these supersymmetric Pati-Salam models. Therefore, we propose a concrete way to obtain the string-scale gauge coupling relations for the generic intersecting D-brane models.

Keywords: D-Branes, String and Brane Phenomenology

ArXiv ePrint: 2212.05875

[1] Corresponding author.

Open Access, © The Authors.
Article funded by SCOAP[3].

https://doi.org/10.1007/JHEP03(2023)210

JHEP03(2023)210

Contents

1 Introduction 1

2 The supersymmetric Pati-Salam models from Type IIA $T^6/(\mathbb{Z}_2 \times \mathbb{Z}_2)$ orientifolds with intersecting D6-branes 3

3 Decoupling of the exotic particles 6

4 String-scale gauge coupling relations 6

4.1 Chiral multiplets from adjoint representations of $SU(4)_C$ and $SU(2)_L$ 9

4.2 The vector-like particles from $\mathcal{N} = 2$ subsector with $k_y > 1$ and $k_2 < 1$ 10

4.3 The vector-like particles from four-dimensional chiral sectors 14

4.4 The vector-like particles from $\mathcal{N} = 2$ subsector with $k_y < 1$ and $k_2 > 1$ 15

5 Discussion and conclusions 19

A Supersymmetric Pati-Salam models 21

B The evolution for the gauge couplings 33

1 Introduction

The three-family $\mathcal{N} = 1$ supersymmetric Pati-Salam models from intersecting D6-branes have been studied extensively since we can generate the Yukawa couplings for the Standard Model (SM) fermions, and break the Pati-Salam gauge symmetry down to the SM gauge symmetry via the D-brane splitting and supersymmetry preserving Higgs mechanism [1–15]. Realizing the SM in D-brane vacua from Orbifold configuration and Gepner configurations were also stuided in [16–29]. However, deriving all the possible Pati-Salam models is a challenging topic due to the large amount of possible wrapping numbers [30–39]. The full landscape of intersecting D-brane models have been under investigation via different perspectives [40–49]. In the Type IIA string theory on $T^6/(\mathbb{Z}_2 \times \mathbb{Z}_2)$ orientifold with intersecting D6-branes, we propose a systematic method to construct all the possible 202752 $\mathcal{N} = 1$ supersymmetric Pati-Salam models [50, 51]. After modding out the equivalent classes, we obtain 33 physical independent models with 33 types of gauge coupling relations. The main idea is to solve the common solutions of three generation conditions, and RR tadpole cancellation conditions iteratively. Thus, we complete the landscape for one particular type of intersecting D-brane models for the first time. However, how to realize the string-scale gauge coupling relations in these models is still a big challenge.

It is well-known that gauge coupling unification can be achieved in the Minimal Supersymmetric SM (MSSM) [52–54], which strongly suggested the Grand Unified Theory (GUT).

JHEP03(2023)210

The unification scale or say GUT scale is around $2 \times 10^{16}\,\text{GeV}$. On the other hand, the string scale is about one order larger. For example, in the weakly coupled heterotic string theory, the string scale M_{string} is given by [55]

$$M_{\text{string}} = g_{\text{string}} \times 5.27 \times 10^{17}\ \text{GeV}\,, \tag{1.1}$$

where g_{string} is string coupling constant. Because $g_{\text{string}} \sim \mathcal{O}(1)$ is an order one coupling constant, we obtain

$$M_{\text{string}} = 5 \times 10^{17}\ \text{GeV}\,. \tag{1.2}$$

And then we have a factor about 25 between the GUT scale and string scale. Thus, how to realize the string-scale gauge coupling unification is an important question in string phenomenology. In principle, the string scale can be low due to the large volume of the extra-dimension [56, 57]. However, recall that the Yang-Mills gauge coupling on the D6-brane stack x at string scale is given by [55]

$$(g^x_{YM})^2 = \frac{\sqrt{8\pi} M_{\text{string}}}{M_{\text{Pl}}} \frac{1}{\prod_{i=1}^3 \sqrt{(n^i_x)^2 \chi_i^{-1} + (2^{-\beta_i} l^i_x)^2 \chi_i}} \tag{1.3}$$

where M_{Pl} is the 4-dimensional Planck scale. To have the proper Yang-Mills coupling $g_{YM} \sim \mathcal{O}(1)$ at order one, the string scale is expected to be closer to the Planck scale M_{Pl} to have proper gauge couplings. Therefore, we set the string scale at $M_{\text{string}} = 5 \times 10^{17}\,\text{GeV}$.

Gauge coupling unification has been studied extensively previously from various physics point of view [58–68]. In general, to achieve the string-scale gauge coupling unification, we need to introduce the new particles at the intermediate scale, such as the SM vector-like particles, and the $\text{SU}(3)_C/\text{SU}(2)_L$ adjoint particles. In particular, we need to obtain these new particles from string model building as well. Moreover, there are two kinds of the string-scale gauge coupling unification: one-step unification [58], and two-step unification for flipped $\text{SU}(5) \times \text{U}(1)_X$ models [59, 62, 64, 65], where the $\text{SU}(3)_C \times \text{SU}(2)_L$ gauge symmetries are unified around the traditional GUT scale, and then $\text{SU}(5) \times \text{U}(1)_X$ gauge symmetries are unified at the string scale.

In the three-family $\mathcal{N} = 1$ supersymmetric Pati-Salam models from the Type IIA string theory on $T^6/(\mathbb{Z}_2 \times \mathbb{Z}_2)$ orientifold with intersecting D6-branes [50, 51], there is one and only one model with gauge coupling unification at the string scale. For the rest 32 models, the gauge couplings for $\text{SU}(4)_C$, $\text{SU}(2)_L$, and $\text{SU}(2)_R$ are not unified at the string scale, and then we have the gauge coupling relations at the string scale as follows

$$k_3 g_a^2 = k_2 g_b^2 = k_Y g_Y^2 = k_y \left(\frac{5}{3} g_Y^2\right) = g_{\text{U}}^2 \sim g_{\text{string}}^2\,, \tag{1.4}$$

where g_a, g_b, and g_Y are respectively the gauge couplings for $\text{SU}(3)_C$, $\text{SU}(2)_L$, and $\text{U}(1)_Y$, and k_3, k_2, k_Y, and k_y are rational numbers. The canonical normalization in SU(5) and SO(10) models give $k_3 = 1$, $k_2 = 1$ and $k_Y = 5/3$. For simplicity, we shall choose $k_3 = 1$.

In the string model building, we generically have exotic particles, and thus need to study how to decouple the exotic particles first. We explain that the exotic particles in most of our models can be decoupled except Model 4, 23, and 32, which have chiral multiplets under

JHEP03(2023)210

$SU(4)_C$ symmetric representation. To realize the string-scale gauge coupling relations, we assume that the exotic particles in these three models can be decoupled as well. Moreover, we can have two scenarios to obtain the string-scale gauge coupling relations: traditional one step, and two steps where the SM gauge symmetry becomes Pati-Salam gauge symmetry at the intermediate scale, and then their gauge couplings satisfy the gauge coupling relations at string scale. In this paper, we only consider the first scenario, and will study the second scenario in the future. Furthermore, we consider the adjoint chiral mulitplets for $SU(4)_C$ and $SU(2)_L$ gauge symmetries, the SM vector-like particles from D6-brane intersections, as well as the vector-like particles from the $\mathcal{N} = 2$ subsector. We show that the gauge coupling relations at string scale can be achieved via two-loop renormalization group equation (RGE) running for all these supersymmetric Pati-Salam models. Therefore, we propose a concrete way to obtain the string-scale gauge coupling relations for the generic intersecting D-brane models.

This paper is organized as follows. In section 2 we first review the construction of supersymmetric Pati-Salam models and present the relevant knowledge. In section 3, we discuss how to decouple the exotic particles. In section 4, we perform the two-loop RGEs of gauge couplings as well as one-loop RGEs of Yukawa couplings. We show that the string-scale gauge coupling relations are achieved after taking into account the contributions from extra vector-like particles. In section 5 we finally conclude the results and make an outlook.

2 The supersymmetric Pati-Salam models from Type IIA $T^6/(\mathbb{Z}_2 \times \mathbb{Z}_2)$ orientifolds with intersecting D6-branes

The supersymmetric Pati-Salam models have been constructed on Type IIA $T^6/(\mathbb{Z}_2 \times \mathbb{Z}_2)$ orientifolds with D6-branes intersecting at generic angles. The orbifold group $\mathbb{Z}_2 \times \mathbb{Z}_2$ results in generators θ and ω and associated with twist vectors $(1/2, -1/2, 0)$ and $(0, 1/2, -1/2)$ respectively. They act on the complex coordinates z_i as [33, 45]

$$\begin{aligned} \theta &: (z_1, z_2, z_3) \mapsto (-z_1, -z_2, z_3)\,, \\ \omega &: (z_1, z_2, z_3) \mapsto (z_1, -z_2, -z_3)\,. \end{aligned} \tag{2.1}$$

The orientifold projection acts by gauging the ΩR symmetry, where Ω is world-sheet parity and R acts on the complex coordinates as

$$R : (z_1, z_2, z_3) \mapsto (\overline{z}_1, \overline{z}_2, \overline{z}_3)\,. \tag{2.2}$$

Overall there are four kinds of orientifold 6-planes (O6-planes) contributes to the actions of ΩR, $\Omega R\theta$, $\Omega R\omega$, and $\Omega R\theta\omega$ respectively [31, 33, 45, 69]. Three stacks of N_a D6-branes wraps on the factorized three-cycles cancelling the RR charges of these O6-planes.

The homology classes of these three cycles are wrapped by the D6-brane stack, taking the form for a rectangular torus as $n_a^i[a_i] + m_a^i[b_i]$ and for a tilted torus as $n_a^i[a_i'] + m_a^i[b_i]$, with $[a_i'] = [a_i] + \frac{1}{2}[b_i]$. We label the generic the generic one cycle by (n_a^i, l_a^i) in terms of the so-called wrapping numbers, with $l_a^i \equiv m_a^i$ for a rectangular and $l_a^i \equiv 2\tilde{m}_a^i = 2m_a^i + n_a^i$ for

JHEP03(2023)210

Orientifold action	O6-Plane	$(n^1,l^1)\times(n^2,l^2)\times(n^3,l^3)$
ΩR	1	$(2^{\beta_1},0)\times(2^{\beta_2},0)\times(2^{\beta_3},0)$
$\Omega R\omega$	2	$(2^{\beta_1},0)\times(0,-2^{\beta_2})\times(0,2^{\beta_3})$
$\Omega R\theta\omega$	3	$(0,-2^{\beta_1})\times(2^{\beta_2},0)\times(0,2^{\beta_3})$
$\Omega R\theta$	4	$(0,-2^{\beta_1})\times(0,2^{\beta_2})\times(2^{\beta_3},0)$

Table 1. The wrapping numbers for four O6-planes.

tilted two-torus respectively. Here $l_a^i - n_a^i$ is even for tilted two-tori, yet odd for rectangular torus. Therefore, the wrapping number for stack a of D6-branes along the cycle are denoted by (n_a^i, l_a^i), while the ΩR images a' stack of N_a D6-branes can be labeled by wrapping numbers $(n_a^i, -l_a^i)$. The homology three-cycles for a stack of D6-branes and its orientifold image a' results in

$$[\Pi_a] = \prod_{i=1}^{3}\left(n_a^i[a_i] + 2^{-\beta_i} l_a^i[b_i]\right),$$
$$[\Pi_{a'}] = \prod_{i=1}^{3}\left(n_a^i[a_i] - 2^{-\beta_i} l_a^i[b_i]\right),$$

in which $\beta_i = 0$ when the i-th two-torus is rectangular while $\beta_i = 1$ for tilted two-torus. Furthermore, the homology three-cycles wrapped by the four O6-planes leads to

$$\begin{aligned}
\Omega R: &\quad [\Pi_{\Omega R}] = 2^3[a_1]\times[a_2]\times[a_3],\\
\Omega R\omega: &\quad [\Pi_{\Omega R\omega}] = -2^{3-\beta_2-\beta_3}[a_1]\times[b_2]\times[b_3],\\
\Omega R\theta\omega: &\quad [\Pi_{\Omega R\theta\omega}] = -2^{3-\beta_1-\beta_3}[b_1]\times[a_2]\times[b_3],\\
\Omega R\theta: &\quad [\Pi_{\Omega R}] = -2^{3-\beta_1-\beta_2}[b_1]\times[b_2]\times[a_3].
\end{aligned} \tag{2.3}$$

Based on these, the RR tadpole cancellation condition provides the restriction rule [13, 14, 45]

$$\begin{aligned}
&-2^k N^{(1)} + \sum_a N_a A_a = -2^k N^{(2)} + \sum_a N_a B_a\\
&= -2^k N^{(3)} + \sum_a N_a C_a = -2^k N^{(4)} + \sum_a N_a D_a = -16
\end{aligned} \tag{2.4}$$

where $2N^{(i)}$ is the number of D6-branes wrapping along the i-th O6-plane (filler branes) and the last term represents the O6-planes with -4 RR charges in D6-brane charge unit. Note that for simplification, we denote $A_a \equiv -n_a^1 n_a^2 n_a^3$, $B_a \equiv n_a^1 l_a^2 l_a^3$, $C_a \equiv l_a^1 n_a^2 l_a^3$, $D_a \equiv l_a^1 l_a^2 n_a^3$, $\tilde{A}_a \equiv -l_a^1 l_a^2 l_a^3$, $\tilde{B}_a \equiv l_a^1 n_a^2 n_a^3$, $\tilde{C}_a \equiv n_a^1 l_a^2 n_a^3$, $\tilde{D}_a \equiv n_a^1 n_a^2 l_a^3$. These filler branes represent the USp group carrying the wrapping numbers with one of the O6-planes as shown in table 1.

To have three family of chiral fermions under $\mathrm{SU}(4)_C \times \mathrm{SU}(2)_L \times \mathrm{SU}(2)_R$ gauge symmetries, further constraints were imposed on the intersection numbers expressed in

JHEP03(2023)210

Sector	Representation
aa	$\mathrm{U}(N_a/2)$ vector multiplet
	3 adjoint chiral multiplets
$ab+ba$	I_{ab} $(\Box_a, \overline{\Box}_b)$ fermions
$ab'+b'a$	$I_{ab'}$ $(\Box_a, \Box_b)$ fermions
$aa'+a'a$	$\frac{1}{2}(I_{aa'}-\frac{1}{2}I_{a,O6})$ $\Box\Box$ fermions
	$\frac{1}{2}(I_{aa'}+\frac{1}{2}I_{a,O6})$ $\begin{smallmatrix}\Box\\\Box\end{smallmatrix}$ fermions

Table 2. General massless particle spectrum for intersecting D6-branes at generic angles.

terms of the wrapping numbers

$$\begin{aligned}
I_{ab} &= [\Pi_a][\Pi_b] = 2^{-k}\prod_{i=1}^{3}(n_a^i l_b^i - n_b^i l_a^i)\,,\\
I_{ab'} &= [\Pi_a][\Pi_{b'}] = -2^{-k}\prod_{i=1}^{3}(n_a^i l_b^i + n_b^i l_a^i)\,,\\
I_{aa'} &= [\Pi_a][\Pi_{a'}] = -2^{3-k}\prod_{i=1}^{3}(n_a^i l_a^i)\,,\\
I_{aO6} &= [\Pi_a][\Pi_{O6}] = 2^{3-k}(-l_a^1 l_a^2 l_a^3 + l_a^1 n_a^2 n_a^3 + n_a^1 l_a^2 n_a^3 + n_a^1 n_a^2 l_a^3)
\end{aligned} \tag{2.5}$$

where $k=\beta_1+\beta_2+\beta_3$ is the total number of tilted two-tori, and $[\Pi_{O6}]=[\Pi_{\Omega R}]+[\Pi_{\Omega R\omega}]+[\Pi_{\Omega R\theta\omega}]+[\Pi_{\Omega R\theta}]$ is the sum of four O6-plane homology three-cycles. And the intersection numbers shall follow

$$I_{ab}+I_{ab'}=3\,,\ I_{ac}=-3\,,\ I_{ac'}=0\,, \tag{2.6}$$

with c and c' exchange as well.

The massless particle spectrum for the supersymmetric Pati-Salam is listed in table 2, where the gauge symmetry results from $\mathbb{Z}_2\times\mathbb{Z}_2$ orbifold projection [60]. The representations refer to $\mathrm{U}(N_a/2)$ when the intersecting D6-branes are of number $N_a=8, N_b=4, N_c=4$. Note that the chiral supermultiplets not only represents the scalars but also the fermions in this supersymmetric constructions. Moreover, positive intersection numbers refer to the left-handed chiral supermultiplets. In our later discussion, some of the introduced particles for gauge coupling unification can be read off from the spectrum table as well.

In addition to the three generation conditions and tadpole cancellation condition, we further need to require $N=1$ supersymmetry preservation in four dimension, with the equality and inequality conditions [5, 33]

$$\begin{aligned}
x_A\tilde{A}_a + x_B\tilde{B}_a + x_C\tilde{C}_a + x_D\tilde{D}_a &= 0,\\
A_a/x_A + B_a/x_B + C_a/x_C + D_a/x_D &< 0,
\end{aligned} \tag{2.7}$$

JHEP03(2023)210

where $x_A = \lambda$, $x_B = \lambda 2^{\beta_2+\beta 3}/\chi_2\chi_3$, $x_C = \lambda 2^{\beta_1+\beta 3}/\chi_1\chi_3$, $x_D = \lambda 2^{\beta_1+\beta 2}/\chi_1\chi_2$. Here $\chi_i = R_i^2/R_i^1$ represent the complex structure moduli of the i-th two-torus, and λ is introduced as a positive parameter to put all the variables A, B, C, D at equal footing.

The supersymmetric Pati-Salam gauge symmetry $\mathrm{SU}(4)_C \times \mathrm{SU}(2)_L \times \mathrm{SU}(2)_R$ can then be broken down to the SM gauge symmetry via the D-brane splitting and Higgs mechanism preserving supersymmetry. Concrete supersymmetric Pati-Salam models have been constructed [46, 47], and such D-brane models have also been investigated with powerful reinforcement machine learning methods [41, 42]. In [50, 51], we for the first time propose a systematic method to construct all the three-family $\mathcal{N} = 1$ supersymmetric Pati-Salam models and conclude that there are in total 202752 models with 33 different gauge coupling relations. Among which, there is one class of models with gauge coupling unification at GUT scale, while the others do not. The absence of gauge coupling unification at the string scale appear be a generic problem. In [50], we propose that by introducing vector-like particles from $\mathcal{N} = 2$ subsector the gauge unification problem may be solved. In particular, the number of these exotic particles are fully determined by the brane intersection number. These additional particles can be decoupled as discussed in [30], and its gauge coupling relation can be realized at string scale via two-loop RGE running. This leads to our exploration that whether this solved for all the supersymmetric Pati-Salam models in general. We will discuss in details for all the 33 representative models.

3 Decoupling of the exotic particles

In the string model building, there exist exotic particles in general. So we need to discuss how to decouple the exotic particles first. In our Pati-Salam models which are given in appendix A, we can decouple most of the exotic particles via Higgs mechanism and instanton effects, etc, except the chiral multiplets under $\mathrm{SU}(4)_C$ symmetric representation. The key point is the gauge anomaly cancellation. First, the chiral multiplets under $\mathrm{SU}(4)_C$ anti-symmetric representation do not contribute to the gauge anomaly. Their mass terms are forbidden by the anomalous U(1) gauge symmetries, and can be generated via the instanton effects [70–72]. Thus, they can be decoupled. Second, for the models without the chiral multiplets under $\mathrm{SU}(4)_C$ symmetric representation, all the exotic particles can be decoupled via Higgs mechanism and instanton effects. For a concrete example, please see [30, 31]. Third, for the models with the chiral multiplets under $\mathrm{SU}(4)_C$ symmetric representation, it seems to us that we cannot decouple the exotic particles. Therefore, we cannot decouple the exotic particles only in Model 4, 23, and 32 in appendix A. To study the gauge coupling unification, we assume the extoic particles in these models can be decoupled as well.

4 String-scale gauge coupling relations

As presented with details in [50, 51], the full list of supersymmetric Pati-Salam models have 33 different gauge coupling relations, see appendix A. In these models, a stack of D6-branes gives the U(4) gauge symmetry, b stack of D6-branes gives the $\mathrm{U}(2)_L$ gauge symmetry, and

JHEP03(2023)210

c stack of D6-branes gives the $\mathrm{U}(2)_R$ gauge symmetry. In particular, there is one class of models with gauge coupling unification at GUT scale. Namely, the strong, weak and hypercharge gauge couplings g_a^2, g_b^2 and $\frac{5}{3}g_Y^2$ satisfy $g_a^2 = g_b^2 = g_c^2 = (\frac{5}{3}g_Y^2) = 4\sqrt{\frac{2}{3}}\pi e^{\phi^4}$, where ϕ^4 represents the dilaton field. However, not all the supersymmetry Pati-Salam models are with gauge coupling unification at GUT scale. To have string-scale gauge coupling relation, we utilize the Renormalization Group Equations (RGEs) evolution [50, 67, 68].

The RGEs for the gauge couplings at the two-loop level are given by [61, 63, 73, 74]

$$\frac{d}{d\ln\mu}g_i = \frac{b_i}{(4\pi)^2}g_i^3 + \frac{g_i^3}{(4\pi)^4}\left[\sum_{j=1}^{3}B_{ij}g_j^2 - \sum_{\alpha=u,d,e}d_i^{\alpha}\mathrm{Tr}\left(h^{\alpha\dagger}h^{\alpha}\right)\right], \tag{4.1}$$

where $g_i (i = 1, 2, 3)$ are the SM gauge couplings and $h^{\alpha} (\alpha = u, d, e)$ are the Yukawa couplings. The coefficients of beta functions in SM [75–78] and supersymmetric models [79–81] are represented by

$$b_{\mathrm{SM}} = \left(\frac{41}{6}\frac{1}{k_Y}, -\frac{19}{6}\frac{1}{k_2}, -7\right), \quad B_{\mathrm{SM}} = \begin{pmatrix} \frac{199}{18}\frac{1}{k_Y^2} & \frac{27}{6}\frac{1}{k_Y k_2} & \frac{44}{3}\frac{1}{k_Y} \\ \frac{3}{2}\frac{1}{k_Y k_2} & \frac{35}{6}\frac{1}{k_2^2} & 12\frac{1}{k_2} \\ \frac{11}{6}\frac{1}{k_Y} & \frac{9}{2}\frac{1}{k_2} & -26 \end{pmatrix}, \tag{4.2}$$

$$d^u_{\mathrm{SM}} = \left(\frac{17}{6}\frac{1}{k_Y}, \frac{3}{2}\frac{1}{k_2}, 2\right), \qquad d^d_{\mathrm{SM}} = 0, \qquad d^e_{\mathrm{SM}} = 0, \tag{4.3}$$

$$b_{\mathrm{SUSY}} = \left(11\frac{1}{k_Y}, \frac{1}{k_2}, -3\right), \qquad B_{\mathrm{SUSY}} = \begin{pmatrix} \frac{199}{9}\frac{1}{k_Y^2} & 9\frac{1}{k_Y k_2} & \frac{88}{3}\frac{1}{k_Y} \\ 3\frac{1}{k_Y k_2} & 25\frac{1}{k_2^2} & 24\frac{1}{k_2} \\ \frac{11}{3}\frac{1}{k_Y} & 9\frac{1}{k_2} & 14 \end{pmatrix}, \tag{4.4}$$

$$d^u_{\mathrm{SUSY}} = \left(\frac{26}{3}\frac{1}{k_Y}, 6\frac{1}{k_2}, 4\right), \qquad d^d_{\mathrm{SUSY}} = 0, \qquad d^e_{\mathrm{SUSY}} = 0, \tag{4.5}$$

where k_Y and k_2 are general normalization factors. By solving the two-loop RGEs for SM gauge couplings, we perform numerically calculations including the one-loop RGEs for Yukawa couplings and taking into account the new physics contributions and threshold. The general one-loop RGEs for Yukawa couplings can be found in [74]. Starting from the electroweak theory, we run the couplings up from Z boson mass scale M_Z to high energies with the boundary conditions for these equations at M_Z as

$$g_1(M_Z) = \sqrt{k_Y}\frac{g_{em}}{\cos\theta_W}\,, \; g_2(M_Z) = \sqrt{k_2}\frac{g_{em}}{\sin\theta_W}\,, \; g_3(M_Z) = \sqrt{4\pi\alpha_s}\,. \tag{4.6}$$

From M_Z up to a supersymmetry breaking scale M_{S}, we consider only the non-supersymmetric SM spectrum including a top quark pole mass at $m_t = 173.34\,\mathrm{GeV}$. From M_{S} scale, we perform the supersymmetric RGEs with all the states including the introduced exotic vector-like particles at M_V. Moreover, the Z boson mass, the Higgs vacuum expectation value, strong coupling constant, fine structure constant, and weak mixing angle at M_Z are choosen to be [82, 83]

$$\begin{aligned} &M_Z = 91.1876\ \mathrm{GeV},\ m_t = 173.34 \pm 0.27(\mathrm{stat}) \pm 0.71(\mathrm{syst})\ \mathrm{GeV},\ v = 174.10\ \mathrm{GeV}, \\ &\alpha_s(M_Z) = 0.1181 \pm 0.0011,\ \alpha_{em}^{-1}(M_Z) = 128.91 \pm 0.02,\ \sin^2\theta_W(M_Z) = 0.23122. \end{aligned} \tag{4.7}$$

JHEP03(2023)210

Based on the experimental lower limits of supersymmetry and gauge hierarchy preservation, we have the supersymmetry breaking scale $M_{\rm S}$ at TeV scale, such as 2.5 TeV or 3.0 TeV. The difference has effect less than 5% on the scale of unification $M_{\rm U}$ while the larger value for $M_{\rm S}$ reduces the unification scale.

Utilizing the current precision electroweak data and setting the supersymmetry breaking scale to be $M_{\rm S} \simeq 3.0\,\text{TeV}$, we study the gauge coupling unification around string scale by solving two-loop RGEs, with

$$M_{\rm U} \sim M_{\rm string} \simeq 5 \times 10^{17}\ \text{GeV}. \tag{4.8}$$

Recall that the generic gauge coupling relations at string scale for supersymmetric Pati-Salam models read

$$g_a^2 = k_2 g_b^2 = k_Y g_Y^2 = g_{\rm U}^2 \sim g_{\rm string}^2, \tag{4.9}$$

where k_Y and k_2 are constants for each model and will determine the value of the mixing angel $\sin\theta_W$ at the string scale. The string-scale gauge coupling relation in the evolution is realized via

$$\alpha_{\rm U}^{-1} \equiv \alpha_1^{-1} = (\alpha_2^{-1} + \alpha_3^{-1})/2 \tag{4.10}$$

with $\alpha_1 \equiv k_Y g_Y^2/4\pi$, $\alpha_2 \equiv k_2 g_b^2/4\pi$, $\alpha_3 \equiv g_a^2/4\pi$, and the accuracy $\Delta = |\alpha_1^{-1} - \alpha_2^{-1}|/\alpha_1^{-1}$ is limited to be less than 1.0%. Here, α_1 and α_2 are traditional gauge couplings if and only if $k_Y = 5/3$ and $k_2 = 1$, respectively.

As discussed in [50], Model 1 in table 8 has a canonical hypercharge normalization $k_Y = 5/3$, and then the gauge coupling unification is naturally achieved at most $M_{\rm U} \sim 2\times10^{16}$ GeV, similar to the predicted unification scale in the MSSM. However, the unification scale is about one order of magnitude smaller than string scale, where the discrepancy can be diminished by the introducing additional vector-like particles [60].

Interestingly, we also find that the precise string-scale gauge coupling relation can be achieved at two-loop level by introducing the extra vector-like particles from $\mathcal{N} = 2$ subsector or four-dimensional chiral sectors in other models. The quantum numbers for the vector-like particles are the same as those of the SM fermions and their Hermitian conjugates. While, the number n_V and the quantum numbers of these particles are highly model dependent and can be determined by brane construction. Particularly, in our calculations, multi-pair of extra particles appears naturally, and we only need to fine tune their masses to unify the gauge coupling near the string scale $M_{\rm string}$. From the numerical results, we find that the mass of these extra particles approach to the string scale as the number of these particles increase.

The quantum numbers of vector-like particles under $\mathrm{SU}(3)_C \times \mathrm{SU}(2)_L \times \mathrm{U}(1)_Y$ and their contributions to one-loop level beta functions [62, 63] are

$$XQ + \overline{XQ} = \left(\mathbf{3}, \mathbf{2}, \frac{\mathbf{1}}{\mathbf{6}}\right) + \left(\bar{\mathbf{3}}, \mathbf{2}, -\frac{\mathbf{1}}{\mathbf{6}}\right), \qquad \Delta b = \left(\frac{1}{5}, 3, 2\right); \tag{4.11}$$

$$XU + \overline{XU} = \left(\mathbf{3}, \mathbf{1}, \frac{\mathbf{2}}{\mathbf{3}}\right) + \left(\bar{\mathbf{3}}, \mathbf{1}, -\frac{\mathbf{2}}{\mathbf{3}}\right), \qquad \Delta b = \left(\frac{8}{5}, 0, 1\right); \tag{4.12}$$

$$XD + \overline{XD} = \left(\mathbf{3}, \mathbf{1}, -\frac{\mathbf{1}}{\mathbf{3}}\right) + \left(\bar{\mathbf{3}}, \mathbf{1}, \frac{\mathbf{1}}{\mathbf{3}}\right), \qquad \Delta b = \left(\frac{2}{5}, 0, 1\right); \tag{4.13}$$

JHEP03(2023)210

$$XL + \overline{XL} = \left(\mathbf{1}, \mathbf{2}, \frac{\mathbf{1}}{\mathbf{2}}\right) + \left(\mathbf{1}, \mathbf{2}, -\frac{\mathbf{1}}{\mathbf{2}}\right), \qquad \Delta b = \left(\frac{3}{5}, 1, 0\right); \tag{4.14}$$

$$XE + \overline{XE} = (\mathbf{1}, \mathbf{1}, \mathbf{1}) + (\mathbf{1}, \mathbf{1}, -\mathbf{1}), \qquad \Delta b = \left(\frac{6}{5}, 0, 0\right); \tag{4.15}$$

$$XG = (\mathbf{8}, \mathbf{1}, \mathbf{0}), \qquad \Delta b = (0, 0, 3); \tag{4.16}$$

$$XW = (\mathbf{1}, \mathbf{3}, \mathbf{0}), \qquad \Delta b = (0, 2, 0). \tag{4.17}$$

In our numerical calculations, the two-loop level beta functions from these particles are used in supersymmetric models from eqs. (B8)-(B11) in [63]. We integrate the renormalization group equations in eq. (4.1) from M_Z up to $M_{\rm string}$ with three sections, from M_Z to $M_{\rm S}$, from $M_{\rm S}$ to M_V, and from M_V to $M_{\rm string}$. The precise energy scale where we realize the string-scale gauge coupling relations depends on the number of the introduced particle, the coefficients b_i, B_{ij} and d_i^α of the beta-function. The values of M_{XG}, M_{XW} are determined by the intersection energy scale of section 2 (from $M_{\rm S}$ to M_V), and section 3 (from M_V to $M_{\rm string}$) in the plot, where these exotic particles are introduced. Thus, the mass of the exotic particles are determined by both the number of the particles, the beta functions and the precise energy scale where we realize the string-scale gauge coupling relations.

Once these particles are included with mass M_V, the evolution of $\alpha_i^{-1}(t)$ is depressed if $\Delta b_i \neq 0$ and the turning point is at $\mu = M_V$. Taking Model 1 as example, we find that there are two bending points for the running of gauge couplings in figure 1; the first one is corresponding to the supersymmetry breaking scale $M_{\rm S} \simeq 3.0\,\text{TeV}$, while the second one corresponds to the introduced particle M_V with chiral multiplets XG and XW obtain the same mass, i.e., $M_{XG} = M_{XW} = M_V$. Recall that $\Delta b_2(XW) = 2$, the plotted lines for α_2^{-1} bend at M_{XW} where the particle XW is introduced. In the same way, the lines for α_3^{-1} bend at the point M_{XG} due to $\Delta b_3(XG) = 3$. Moreover, the degree of depression will increase as Δb_i increases. That's to say, the inverse hypercharge coupling α_1^{-1} decreases more rapidly in models with the particles $XU + \overline{XU}$ than that in models with $XD + \overline{XD}$. And the depression of the inverse strong coupling α_3^{-1} from both pairs of vector-like particles are the same. Note that when both particles $XU + \overline{XU}$ and $XD + \overline{XD}$ are added, there will be two bending points at $M_{\rm S}$ and M_V as these particles have the same mass $M_V = M_{XU} = M_{XD}$, while there will be three bending points at $M_{\rm S}$, M_{XU} and M_{XD} as the mass of these particles are different.

4.1 Chiral multiplets from adjoint representations of $\mathrm{SU}(4)_C$ and $\mathrm{SU}(2)_L$

For the Model 1 with $k_y = k_2 = 1$, the gauge couplings naturally unifies at the traditional GUT scale, one order of magnitude smaller than the string scale. Instead of introducing the vector-like particle from a $\mathcal{N} = 2$ subsector, we consider up to three chiral multiplets in the adjoint representations of $\mathrm{SU}(4)_C$ and $\mathrm{SU}(2)_L$ with masses $M_V (V = XG \text{ and } XW)$. These two particles XG and XW arise from the aa and bb sectors in the spectrum table 2, and thus the maximum number is 3. The gauge couplings can be unified at close to the string scale, $M_{\rm U} = 5.0 \times 10^{17}\,\text{GeV}$. The two-loop RGE running for the guage couplings are shown in figure 1. As the number of particles increases, the mass of the particles increases and approaches the string scale. Moreover, the splitting between the XW and XG masses

JHEP03(2023)210

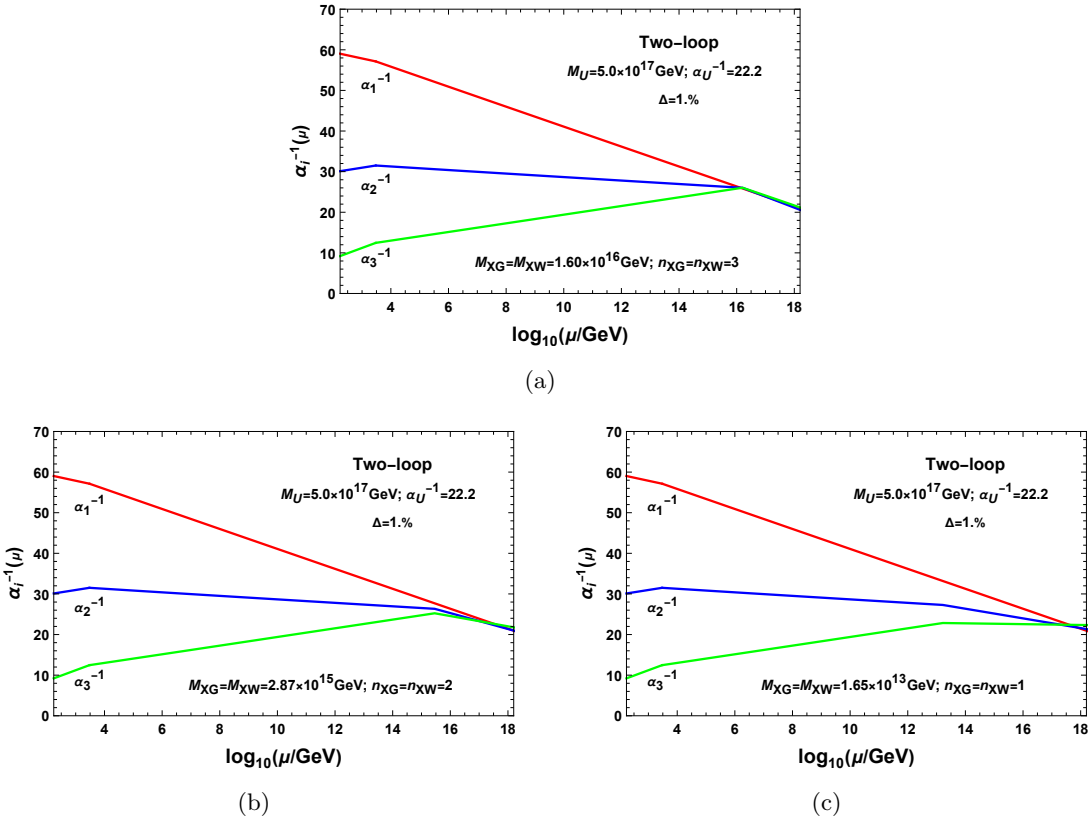

Figure 1. Two-loop evolution of gauge couplings for the **Model 1** with vector-like particles. In the model, $k_Y = 1 \times \frac{5}{3}$ and $k_2 = 1$. The string-scale gauge coupling relations can be achieved by adding $3(XG + XW)$ (a), $2(XG + XW)$ (b) and $(XG + XW)$ (c).

will be reduced. Thus in the following calculations, we choose to add 3 $(XG + XW)$. The energy scale, number of the particles, and the mass of the particles for the Model 1–12 are shown in table 3. Above M_V, the running of $\mathrm{SU}(3)_C$ coupling and $\mathrm{SU}(2)_L$ coupling are reducing due to the non-zero beta functions $\Delta b_3(XG)$ and $\Delta b_2(XW)$. For the models with $k_y > 1$ and $k_2 < 1$, the string-scale gauge coupling relation can also be achieved by adding $XW + XG$ from adjoint representation of SU(4) and SU(2). The two-loop RGE running for the gauge couplings of the Model 2 is plotted in figure 2. Here we include the contributions from $3(XW + XG)$ to reduce the mass splitting of these added particles. And the two-loop RGE running of the gauge couplings for Model 3–5 are shown in figures 3, 4, 5, for Model 6–12 in figures 11, 12, 13, 14, 15, 16, 17 in appendix B, for Model 13–14 in figures 6 and 7.

4.2 The vector-like particles from $\mathcal{N} = 2$ subsector with $k_y > 1$ and $k_2 < 1$

For the models like Model 2 in table 9, the evolution of $\alpha_1^{-1}(\mu)$ is depressed when $k_y > 1$ and the evolution of $\alpha_2^{-1}(t)$ is raised when $k_2 < 1$. They induces that the intersection point of $\alpha_1^{-1}(t)$ and $\alpha_3^{-1}(t)$ lines is below the line of $\alpha_2^{-1}(t)$, as illustrated in figure 2(a). In this case, to get an string-scale gauge coupling relation, we need introduce extra particles $XQ + \overline{XQ}$ or XW as well as XG into the models, which will mainly modify the evolution

JHEP03(2023)210

Model No.	k_y	k_2	n_V	M_{XG}(GeV)	M_{XW}(GeV)	$M_{\rm U}$(GeV)
1	1	1	3	1.60×10^{16}	1.60×10^{16}	5.00×10^{17}
			2	2.87×10^{15}	2.87×10^{15}	5.00×10^{17}
			1	1.65×10^{13}	1.65×10^{13}	5.00×10^{17}
2	85/61	4/9	3	2.76×10^{14}	7.84×10^{9}	5.00×10^{17}
3	65/44	1/2	3	1.28×10^{14}	1.34×10^{10}	5.00×10^{17}
4	35/32	5/6	3	3.50×10^{15}	1.23×10^{14}	5.00×10^{17}
5	10/7	2/3	3	2.87×10^{14}	2.00×10^{11}	5.85×10^{17}
6	11/8	5/6	3	3.13×10^{14}	3.06×10^{12}	5.00×10^{17}
7	25/19	1	3	3.98×10^{14}	1.19×10^{14}	5.00×10^{17}
8	10/7	1	3	1.73×10^{14}	3.17×10^{13}	5.00×10^{17}
9	11/8	1/6	3	2.63×10^{14}	2.06×10^{8}	5.00×10^{17}
10	50/47	4/9	3	5.10×10^{15}	6.90×10^{10}	5.00×10^{17}
11	1	1/3	3	1.21×10^{16}	1.18×10^{12}	5.00×10^{17}
12	35/32	1/6	3	1.22×10^{16}	4.49×10^{8}	5.00×10^{17}
13	11/8	5/14	3	3.18×10^{14}	2.45×10^{9}	5.00×10^{17}
14	35/32	35/66	3	4.62×10^{14}	2.33×10^{11}	5.00×10^{17}

Table 3. String-scale gauge coupling relations achieved with $XG+XW$, from adjoint representation of SU(4) and SU(2).

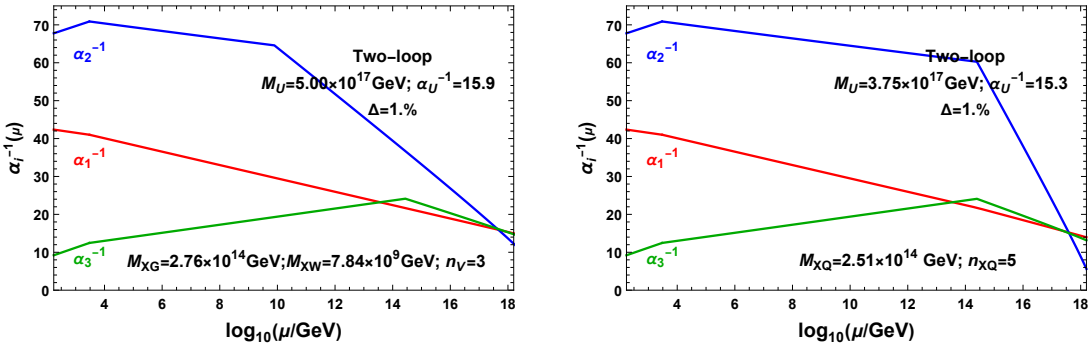

(a) (b)

Figure 2. Two-loop evolution of gauge couplings for the **Model 2** with vector-like particles. In the model, $k_Y = \frac{85}{61} \times \frac{5}{3}$ and $k_2 = \frac{4}{9}$. The string-scale gauge coupling relations can be achieved by adding $3(XW + XG)$ (a) and $5(XQ + \overline{XQ})$ (b).

JHEP03(2023)210

Model No.	k_y	k_2	n_{XQ}	M_{XQ}(GeV)			$M_{\rm U}$(GeV)
2	85/61	4/9	5	2.51×10^{14}			3.75×10^{17}
3	65/44	1/2	3	1.26×10^{12}			1.81×10^{17}
4	25/32	5/6	7	1.07×10^{16}			1.09×10^{17}
Model No.	k_y	k_2	n_{XQ}	M_{XQ}(GeV)	n_{XG}	M_{XG}(GeV)	$M_{\rm U}$(GeV)
5	10/7	2/3	5	1.03×10^{15}	3	1.18×10^{17}	5.00×10^{17}
6	11/8	5/6	7	1.51×10^{16}	3	3.69×10^{16}	5.00×10^{17}
7	25/19	1	3	1.43×10^{14}	3	1.41×10^{16}	5.00×10^{17}
8	10/7	1	3	4.73×10^{14}	3	1.50×10^{16}	5.00×10^{17}
Model No.	k_y	k_2	n_{XQ}	M_{XQ}(GeV)	n_{XW}	M_{XW}(GeV)	$M_{\rm U}$(GeV)
9	11/8	1/6	5	3.84×10^{14}	3	8.10×10^{15}	5.00×10^{17}
10	50/47	4/9	5	5.13×10^{15}	3	4.39×10^{16}	5.00×10^{17}
11	1	1/3	5	1.60×10^{16}	3	4.12×10^{13}	5.00×10^{17}
12	35/32	1/6	5	1.66×10^{16}	3	1.44×10^{12}	5.00×10^{17}

Table 4. String-scale gauge coupling relations achieved by adding vector-like particles $XQ + \overline{XQ}$ as well as XG or XW, from $\mathcal{N} = 2$ subsector. The number of vector-like particles are defined by the intersection number on a and b stacks, $n_v = I_{ab}$.

of the electroweak and strong couplings without substantially affecting the U(1) coupling. This is owing to the large contributions to Δb_2 and Δb_3, rather relatively small contributions to Δb_1. So as the energy rises from mass scale M_{XQ}, α_2^{-1} and α_3^{-1} reduce rapidly. Therefore, string-scale gauge coupling relations are achieved near $M_{\rm U} = 3.75 \times 10^{17}$ GeV by adding 5 sets of $XQ + \overline{XQ}$ at $M_{XQ} = 2.51 \times 10^{14}$ GeV. The evolution of gauge couplings for Model 2 with $k_y = 85/61$ and $k_2 = 4/9$ is shown in figure 2(b) and the energy scale, the number and mass of the added vector-like particles $XQ + \overline{XQ}$ are list in table 4.

Similarly, for Model 3 and 4, the non-canonical constants are $k_y = 65/44,\ k_2 = 1/2$ and $k_y = 25/32,\ k_2 = 5/6$. The string-scale gauge coupling relation are also achieved by bringing particles $XQ+\overline{XQ}$ into Model 3 at 1.26×10^{12} GeV and Model 4 at 1.07×10^{16} GeV, respectively. The evolution of gauge couplings are shown in figures 3 and 4, in which the number of pairs of the new vector-like particles is 3 and 7, respectively. We note that the mass of the extra particles is related to the number of pairs of particles. As the number increases, the mass scale is pushed up to the high energy scale and thus the vector-like particles decay at high energy scale.

Of course, the number of these extra vector-like particles is not random, yet from brane constructions. From eqs. (4.11) and (4.17), the quantum numbers of these particles under $\mathrm{SU}(3)_C \times \mathrm{SU}(2)_L \times \mathrm{U}(1)_Y$ are $XQ = (3, 2, 1/6)$, and $\overline{XQ} = (\bar{3}, 2, -1/6)$. In the

JHEP03(2023)210

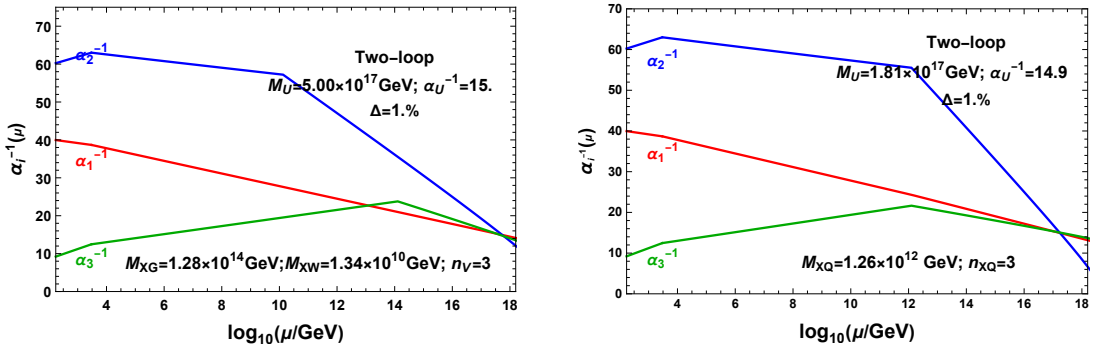

(a) (b)

Figure 3. Two-loop evolution of gauge couplings for the **Model 3** with vector-like particles. In the model, $k_Y = \frac{65}{44} \times \frac{5}{3}$ and $k_2 = \frac{1}{2}$. The string-scale gauge coupling relations can be achieved by adding $3(XW + XG)$ (a) and $3(XQ + \overline{XQ})$ (b).

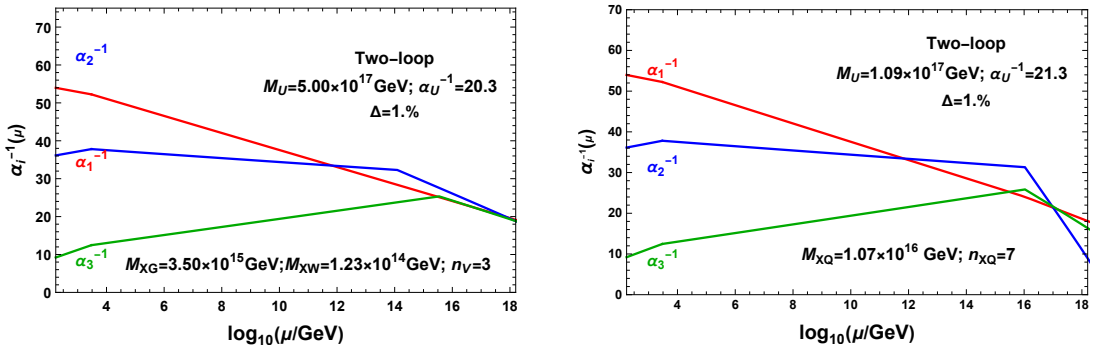

(a) (b)

Figure 4. Two-loop evolution of gauge couplings for the **Model 4** with vector-like particles. In the model, $k_Y = \frac{35}{32} \times \frac{5}{3}$ and $k_2 = \frac{5}{6}$. The string-scale gauge coupling relations can be achieved by adding $3(XW + XG)$ (a) and $7(XQ + \overline{XQ})$ (b).

supersymmetric Pati-Salam models, these vector-like particles $(XQ + \overline{XQ})$ arise from the intersections between a and b stacks of D6-branes or a and b' stacks of D6-brane. The particle XW arise from bb sector of the adjoint representation of $\mathrm{SU}(2)_L$.

Base on the brane construction, the number of vector-like particles $(XQ + \overline{XQ})$ can be determined by the intersection number of the a and b stacks of D6-brane, I_{ab}, or a and b' stacks of D6-brane, $I_{ab'}$. For example, the intersection number is $I_{ab'} = -2^0(4+1)(1) = -5$ in Model 2 (table 9) and the corresponding number of the additional particles $(XQ + \overline{XQ})$ is 5. If the wrapping numbers (n_a^i, l_a^i) and (n_b^i, l_b^i) have the same value, indicating that the D6-branes warpping on the $i-$ torus are parallel to each other. Therefore, there is no intersection on the i-torus, but only on the other two torus. From table 10, we see that (n_a^3, l_a^3) and (n_b^3, l_b^3) for Model 3 are the same, thus the intersection number of the a and b stacks are only calculated on the first two torus, i.e., $I_{ab} = 2^0(-2-5)(1) = 7$. Namely, 7 pairs of $XQ + \overline{XQ}$ naturally arise from brane intersection.

JHEP03(2023)210

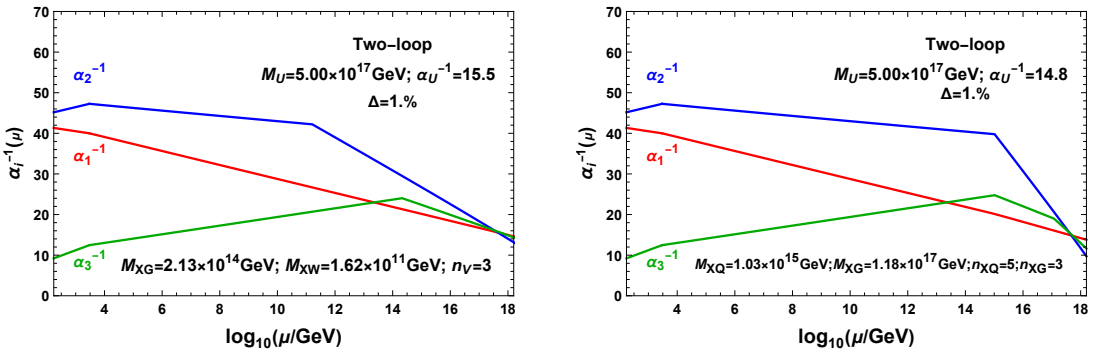

(a) (b)

Figure 5. Two-loop evolution of gauge couplings for the **Model 5** with vector-like particles. In the model, $k_Y = \frac{10}{7} \times \frac{5}{3}$ and $k_2 = \frac{2}{3}$. The string-scale gauge coupling relations can be achieved by adding $3(XW + XG)$ (a) and $5(XQ + \overline{XQ}) + 3XG$ (b).

Based on the calculations, we know that the energy scale is pushed up to high energy scale as k_y or k_2 deceases. Thus, for the models with $k_y > 1$, to obtain a string-scale gauge coupling relation, the constant k_2 of the model should be smaller than 1/2. Otherwise, the gauge couplings are unified at an intermediate energy scale $10^{14} - 10^{16}$ GeV, little smaller than the string scale. For Model 5 with $k_y > 1$ and $k_2 > 1/2$, the gauge coupling relation can be achieved at the string scale $M_{\rm U} \simeq 5 \times 10^{17}$ GeV by adding 5 pairs of $XQ + \overline{XQ}$ and 3 XG. For Models 5–8, the parameter k_y is almost equal. And the parameter k_2 in Models 6–8 is larger than that in Model 5. Thus, the energy scale is smaller than that in Model 5. To increase the energy scale, we also need to introduce adjoint particle XG for Models 6–8. The evolution of gauge couplings for Models 5–8 with vector-like particles and XG are presented in figures 5, 11, 12 and 13, respectively. However, the parameter k_2 should not be too small either, as this would realize the gauge coupling relation beyond Planck level, where we do not know how to quantize gravity. This thorny issue will arise when we deal with models 9–12. The evolution of gauge couplings for Models 9–12 is shown in figures 14, 15, 16, 17, in appendix B. Note that the U(1) and strong couplings are unified below the Planck scale. We find that the electroweak coupling can be unified with other two couplings below the Planck scale by introducing XW, which only affects the running of electroweak coupling due to $\Delta b_2 \neq 0$. Take Model 11 as example, the U(1) and strong couplings are unified at 1×10^{18} GeV, while the gauge couplings are unified at same energy scale after introducing 3 XW at 1.4×10^{12} GeV. To obtain string-scale gauge coupling relation for these models, the additional particles are $XQ + \overline{XQ}$ as well as XW. The numbers and the masses of these particles are given in the gauge revolution figures.

4.3 The vector-like particles from four-dimensional chiral sectors

On the other hand, Model 13 in table 20 with $k_y = 11/8$ and $k_2 = 5/14$ also can achieve string-scale gauge coupling relation while the vector-like particles $XQ + \overline{XQ}$ are added. The number of these vector-like particles are defined by the fundamental minus anti-fundamental representation, with $6 - 3 \equiv 3$. The evolution of gauge couplings for the model are shown in

JHEP03(2023)210

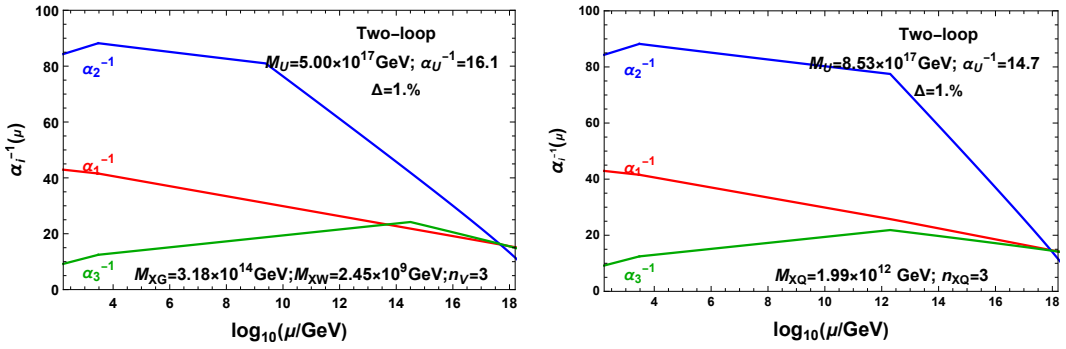

(a) (b)

Figure 6. Two-loop evolution of gauge couplings for the **Model 13** with vector-like particles. In the model, $k_Y = \frac{11}{8} \times \frac{5}{3}$ and $k_2 = \frac{5}{14}$. The string-scale gauge coupling relations can be achieved by adding $3(XW + XG)$ (a) and $3(XQ + \overline{XQ})$ (b).

Model No.	k_y	k_2	n_{XQ}	M_{XQ} (GeV)	n_{XW}	M_{XW}	$M_{\rm U}$(GeV)
13	11/8	5/14	3	1.99×10^{12}			8.53×10^{17}
14	35/32	35/66	3	1.525×10^{14}	1	1.525×10^{14}	5.00×10^{17}
				1.34×10^{14}	2	1.30×10^{16}	
				1.70×10^{14}	3	2.75×10^{16}	

Table 5. String-scale gauge coupling relations achieved by adding vector-like particles $XQ + \overline{XQ}$ from four-dimensional chiral sectors as well as XW from bb sector.

figure 6. The energy scale is around 8×10^{17} GeV, and the new vector-like particles decay to the corresponding SM fermions below $M_{XQ} \simeq 2 \times 10^{12}$ GeV. The number and mass of new vector-like particles are also shown in the plot. Unlike Model 2–12 discussed above, the vector-like particles entered in this model come from the four-dimensional chiral sector of the brane building. Furthermore, Model 14 in table 21 with $k_y = 35/32$ and $k_2 = 35/66$, also have a energy scale at 1.8×10^{18} GeV moderately larger than the string scale. As discussed before, the contributions of the particle XW are also included in this model. The particle XW comes from the bb sector of the brane configuration. Comparison of the masses of vector-like particles with different XW numbers shows that the mass splitting between XQ and XW increases with the number of XW. When XW(s) is (are) added, the XW acquires the same mass as the XQ from the naturalness point of view. Therefore, the number of XW needs to be carefully chosen in order to reduce their mass splitting. The evolution of gauge couplings for the model are shown in figure 7. The string-scale gauge coupling relations for Model 13–14 are listed in table. 5.

4.4 The vector-like particles from $\mathcal{N} = 2$ subsector with $k_y < 1$ and $k_2 > 1$

On the contrary, when $k_y < 1$ or $k_2 > 1$, the intersection of α_1^{-1} and α_3^{-1} lines lies above the line of $\alpha_2^{-1}(t)$, which can be seen from Model 15 without vector-like particle in figure 8(a).

JHEP03(2023)210

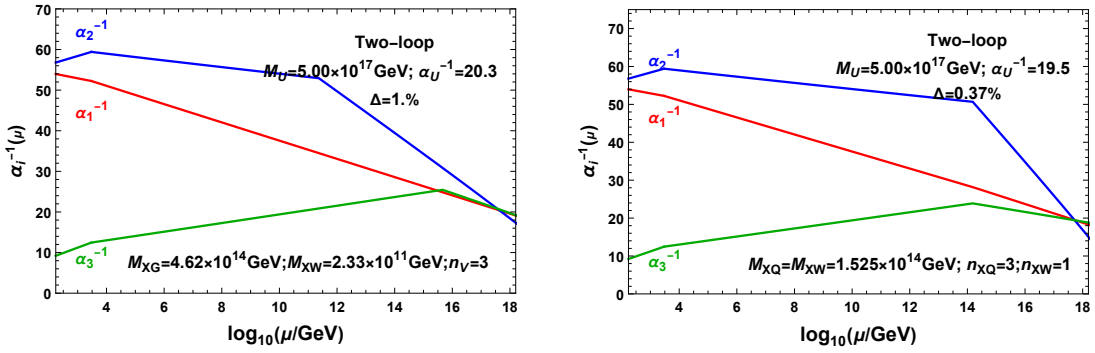

(a) (b)

Figure 7. Two-loop evolution of gauge couplings for the **Model 14** with vector-like particles. In the model, $k_Y = \frac{35}{32} \times \frac{5}{3}$ and $k_2 = \frac{35}{66}$. The string-scale gauge coupling relation can be achieved by adding $3(XW + XG)$ (a) and $3(XQ + \overline{XQ}) + XW$ (b).

And thus, if we want to push or pull back the energy scale to string scale $M_{\rm string}$, the extra particles arise from $\mathcal{N} = 2$ subsector, like $(XD + \overline{XD})$ and $(XU + \overline{XU})$, which will modify the evolution of the U(1) and strong couplings rather than electroweak coupling. This is due to the non-zero Δb_1 and Δb_3. As we mentioned earlier, since $\Delta b_1(XD) < \Delta b_1(XU)$, the suppression of α_1^{-1} is stronger in the models with $XD + \overline{XD}$ particles than that with $XU + \overline{XU}$ particles. And thus, the energy scale is higher in the models with $(XD + \overline{XD})$ than that with $(XU + \overline{XU})$. Of course, in some models with much smaller k_y or much larger k_2, we need to add both particles to obtain the string-scale gauge coupling relation. Additional, there is mass splitting between these two particles. The energy scale, the number and mass of the added vector-like particles $(XD + \overline{XD})$ and $(XU + \overline{XU})$ are list in table 6. Another vector-like particle $(XE + \overline{XE})$, from $\mathcal{N} = 2$ subsector, will only modify the running of the U(1) coupling due to $\Delta b_1(XE) \neq 0$. When used with XG, from aa sectors, the results are similar or even better than those of $(XD + \overline{XD})$ and $(XU + \overline{XU})$. The energy scale, the number and mass of the added vector-like particles $(XE + \overline{XE})$ and XG are list in table 7.

Base on the brane construction, the number of vector-like particles $(XD + \overline{XD})$, $(XU + \overline{XU})$ and $(XE + \overline{XE})$ can be determined by the intersection number of the a and c stacks I_{ac}. For example, the intersection number is $I_{ac} = 2^0(1)(-2-5) = -7$ in Model 15 (table 22) and the corresponding number of the vector-like particles $(XD + \overline{XD})$ is 7. In this model, the wrapping numbers (n_a^3, l_a^3) and (n_c^3, l_c^3) have the same value yet with opposite sign, indicating that the D6-branes warpping on the third torus are parallel to each other. Therefore, the intersection number of the a and c stacks are only calculated on the first two torus.

For Model 15, the parameters $k_y = 25/28$ and $k_2 = 7/6$ slightly deviate from 1, the string-scale gauge coupling relation can be achieved by introducing vector-like particles, e.g., a string-scale gauge coupling relation obtained at $M_{\rm U} = 7.22 \times 10^{17}$ GeV by adding 7 pair of $XD + \overline{XD}$. During the evolution of gauge couplings, the extra particles are introduced around 5.6×10^{15} GeV. While, when the same number of vector-like particles $XU + \overline{XU}$ are

JHEP03(2023)210

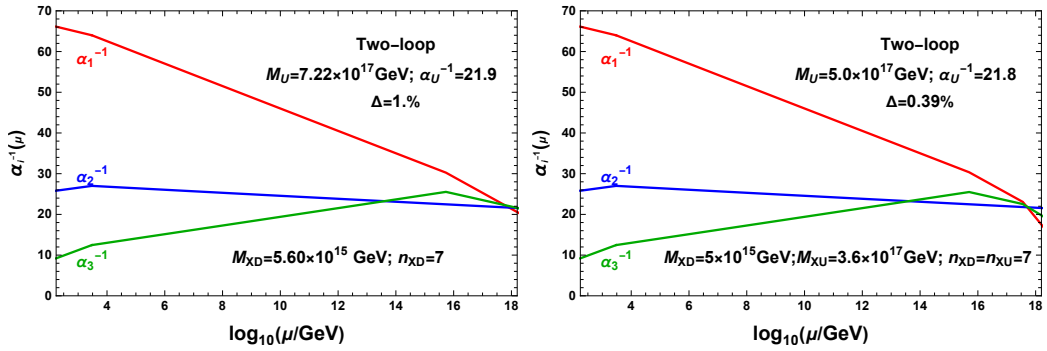

(a) (b)

Figure 8. Two-loop evolution of gauge couplings for the **Model 15** with vector-like particles. In the model, $k_Y = \frac{25}{28} \times \frac{5}{3}$ and $k_2 = \frac{7}{6}$. The string-scale gauge coupling relation can be achieved by adding $7(XD + \overline{XD})$ (a) as well as $7(XU + \overline{XE})$ (b).

Model No.	k_y	k_2	n_v	M_{XD}(GeV)	M_{XU}(GeV)	$M_{\rm U}$(GeV)
15	25/28	7/6	7	5.60×10^{16}		7.22×10^{17}
16	10/7	2	3	6.9×10^{4}		1.2×10^{17}
17	1/4	11/6	3		3.70×10^{10}	1.43×10^{17}
18	10/7	18/5	3	8.90×10^{3}	1.60×10^{14}	3.25×10^{17}
19	1	5/3	3	2.00×10^{8}	1.40×10^{17}	4.90×10^{17}
20	1	2	3	3.71×10^{7}	1.05×10^{14}	5.00×10^{17}
21	1	54/19	3	2.13×10^{6}	2.43×10^{13}	5.00×10^{17}
22	1	9/5	3	1.80×10^{8}	6.20×10^{15}	5.50×10^{17}
23	5/8	13/6	3	8.20×10^{10}	8.20×10^{10}	3.60×10^{17}
24	10/13	2	5	9.00×10^{12}	8.00×10^{14}	5.58×10^{17}
25	4/7	17/9	5	1.08×10^{14}	1.08×10^{14}	6.61×10^{17}
26	25/28	11/6	7	8.71×10^{13}	2.75×10^{15}	3.43×10^{17}

Table 6. String-scale gauge coupling relations achieved by adding vector-like particles $XD + \overline{XD}$ or/and $XU + \overline{XU}$ from $\mathcal{N} = 2$ subsector. The number of vector-like particles are defined by the intersection number on a and c stacks, $n_v = I_{ac}$.

added at 7×10^{14} GeV, a GUT scale gauge coupling relation is obtained at 1.8×10^{16} GeV. Furthermore, adding both particles and fine-tuning their masses, $M_{\rm U} = 5.0 \times 10^{17}$ GeV can be achieved and the accuracy is as small as 0.39%. The evolution of gauge couplings for the model with vector-like particles are show in figure 8. Models 16 is similar and the evolution of their gauge coupling is shown in figure 18.

For Model 17, the parameters $k_y = 1/4$ and $k_2 = 11/6$ deviate significantly from 1, the evolution for U(1) coupling α_1^{-1} cannot intersect the other two couplings. In order to

JHEP03(2023)210

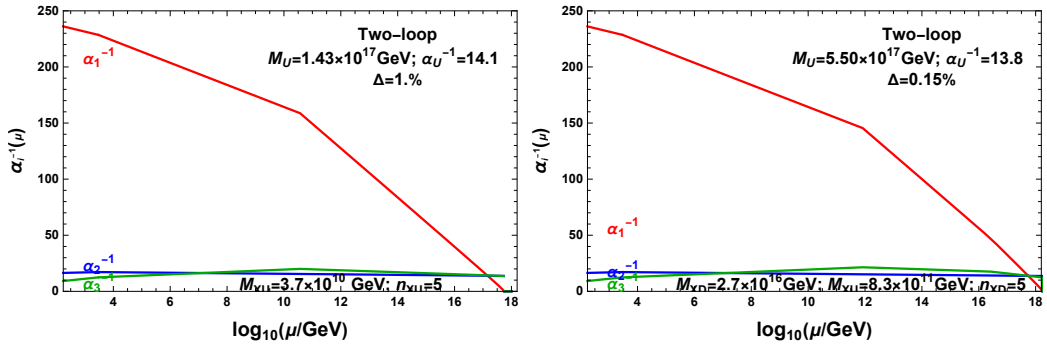

(a) (b)

Figure 9. Two-loop evolution of gauge couplings for the **Model 17** with vector-like particles. In the model, $k_Y = \frac{1}{4} \times \frac{5}{3}$ and $k_2 = \frac{11}{6}$. The string-scale gauge coupling relations can be achieved by adding $5(XU + \overline{XU})$ (a) as well as $5(XD + \overline{XD})$ (b).

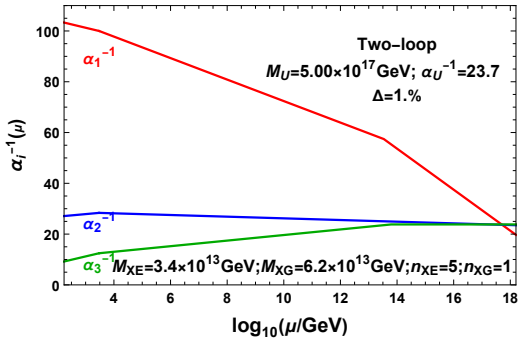

Figure 10. Two-loop evolution of gauge couplings for the **Model 27** with vector-like particles. In this model, $k_Y = \frac{4}{9} \times \frac{5}{3}$ and $k_2 = \frac{10}{9}$. The string-scale gauge coupling relations can be achieved by adding $5(XE + \overline{XE}) + XG$ around 10^{13} GeV.

get a string-scale gauge coupling relation, we choose to introduce 5 pairs of $XU + \overline{XU}$ at 3.7×10^{10} GeV. The evolution of gauge couplings for this model without and with vector-like particles are shown in figure 9. Note that the energy scale is pushed above the Planck scale by adding $XD + \overline{XD}$. This is common for models with parameters $k_y \ll 1$ and $k_2 \gg 1$. In such case, we introduce additional $XU + \overline{XU}$ particles to pull the energy scale to intermediate scales $10^{14} - 10^{15}$ GeV. Therefore, a string-scale gauge coupling relation can be achieved by adding both $XD + \overline{XD}$ and $XU + \overline{XU}$ and fine-tuning their masses. The masses for these vector-like particles M_V and the energy scales for Models 18–26 are listed in table 6, and the corresponding evolution of gauge couplings are illustrated in figures 19, 20 and 21, in appendix B.

However, if one and only one of parameters k_y and k_2 deviates significantly from 1, the situations are more complicated. When $k_2 \sim 1$ and $k_y \ll 1$, by adding $(XD + \overline{XD})$ and $(XU + \overline{XU})$ the string-scale gauge coupling realtion is pushed too high and above the Planck scale. Another kind of vector-like particles $(XE + \overline{XE})$ from $\mathcal{N} = 2$ subsector as well as XG from aa sector are added in these models to obtain the string-scale gauge

JHEP03(2023)210

Model No.	k_y	k_2	n_{XE}	M_{XE}(GeV)	n_{XG}	M_{XG}(GeV)	$M_{\rm U}$(GeV)
27	4/9	10/9	5	3.40×10^{13}	1	6.20×10^{13}	5.00×10^{17}
28	5/11	1	5	5.50×10^{12}	1	3.80×10^{15}	5.00×10^{17}
29	1/4	7/6	5	7.80×10^{9}	1	1.70×10^{12}	5.00×10^{17}
30	10/7	27/11	3	1.51×10^{12}	3	3.11×10^{12}	5.00×10^{17}
31	5/3	13/5	3	1.36×10^{13}	3	4.98×10^{12}	5.00×10^{17}
32	7/4	21/10	3	5.72×10^{16}	3	1.94×10^{13}	5.00×10^{17}
33	2	26/5	3	3.44×10^{8}	2	4.92×10^{7}	5.00×10^{17}

Table 7. String-scale gauge coupling relations achieved by adding vector-like particles $XE + \overline{XE}$ from $\mathcal{N} = 2$ subsector and XG from the adjiont sector. The number of $XE + \overline{XE}$ is defined by the intersection number on a and c stacks, $n_{XE} = I_{ac}$.

coupling relations. For Model 27 with $k_y = 4/9$ and $k_2 = 10/9$, the gauge coupling relation can be realized at the string scale $M_{\rm U} = 5.00 \times 10^{17}$ GeV by adding $5(XE + \overline{XE}) + XG$ at 10^{13} GeV. The details for Model 27, and 28–29 are listed in table 7 and the corresponding running of gauge couplings are plotted in figures 10, and 22.

For Model 30–33, even the parameter k_y is greater than 1, the intersection of α_1^{-1} and α_3^{-1} is still above the line of α_2^{-1} because k_2 is too large. Thus, to get a string-scale gauge coupling relation, the vector-like particles added are $(XE + \overline{XE})$ from $\mathcal{N} = 2$ subsector as well as XG from aa sectors. For Model 30, a string-scale gauge coupling relation is achieved at 5.00×10^{17} GeV by fine-tuning the masses of XE and XG as well as the number of XG. The appropriate number of XG are chosen to reduce the mass splitting. For Model 30–33, the energy scales, number and mass of these additional particles are listed in table 7 and the corresponding evolution are figured in figure 23 in appendix B.

5 Discussion and conclusions

In [51], we have constructed all the three-family $\mathcal{N} = 1$ supersymmetric Pati-Salam models in the Type IIA string theory on $T^6/(\mathbb{Z}_2 \times \mathbb{Z}_2)$ orientifold with intersecting D6-branes, and obtained all the possible 33 independent models in total. However, how to realize the string-scale gauge coupling relations for these models is still a big challenge. In this paper, we systematically studied the string-scale gauge coupling relations for all these models. First, we discussed how to decouple the exotic particles in these models. Second, utilizing the two-loop RGEs revolutions, we obtained string-scale gauge coupling relations by introducing additional particles from the adjoint representations of $\mathrm{SU}(4)_C$ and $\mathrm{SU}(2)_L$ gauge symmetries, SM vector-like particles from four-dimensional chiral sectors, as well as vector-like particles from $\mathcal{N} = 2$ subsector. Although most of these supersymmetric Pati-Salam models do not directly have traditional gauge coupling unification at string scale, their gauge coupling relations can indeed be realized at string scale. Therefore, we solved the string-scale gauge coupling relation problems for the generic intersecting D6-brane

JHEP03(2023)210

models. It seems to us that this systematic method can be applied to the other intersecting D-brane model building as well.

Acknowledgments

TL is supported in part by the National Key Research and Development Program of China Grant No. 2020YFC2201504, by the Projects No. 11875062, No. 11947302, No. 12047503, and No. 12275333 supported by the National Natural Science Foundation of China, by the Key Research Program of the Chinese Academy of Sciences, Grant NO. XDPB15, by the Scientific Instrument Developing Project of the Chinese Academy of Sciences, Grant No. YJKYYQ20190049, and by the International Partnership Program of Chinese Academy of Sciences for Grand Challenges, Grant No. 112311KYSB20210012. RS is supported by KIAS Individual Grant PG080701 and PG080704.

JHEP03(2023)210

A Supersymmetric Pati-Salam models

In this appendix, we present the supersymmetric Pati-Salam models with 33 types of allowed gauge coupling relations on the landscape of supersymmetric Pati-Salam model building.

Model 1	$\mathrm{U}(4)\times\mathrm{U}(2)_L\times\mathrm{U}(2)_R\times\mathrm{USp}(2)^4$											
stack	N	$(n^1,l^1)\times(n^2,l^2)\times(n^3,l^3)$	$n_{\square\square}$	$n_{\begin{smallmatrix}\square\\\square\end{smallmatrix}}$	b	b'	c	c'	1	2	3	4
a	8	$(1,1)\times(1,0)\times(1,-1)$	0	0	3	0	0	-3	0	1	0	-1
b	4	$(-1,0)\times(-1,3)\times(1,1)$	2	-2	—	—	0	0	0	0	-3	1
c	4	$(0,1)\times(-1,3)\times(-1,1)$	2	-2	—	—	—	—	-3	1	0	0
1	2	$(1,0)\times(1,0)\times(2,0)$	$x_A=\frac{1}{3}x_B=x_C=\frac{1}{3}x_D$									
2	2	$(1,0)\times(0,-1)\times(0,2)$	$\beta_1^g=\beta_2^g=\beta_3^g=\beta_4^g=-3$									
3	2	$(0,-1)\times(1,0)\times(0,2)$	$\chi_1=1,\ \chi_2=\frac{1}{3},\ \chi_3=2$									
4	2	$(0,-1)\times(0,1)\times(2,0)$										

Table 8. D6-brane configurations and intersection numbers of Model 1, and its gauge coupling relation is $g_a^2=g_b^2=g_c^2=(\frac{5}{3}g_Y^2)=4\sqrt{\frac{2}{3}}\pi e^{\phi^4}$.

Model 2	$\mathrm{U}(4)\times\mathrm{U}(2)_L\times\mathrm{U}(2)_R\times\mathrm{USp}(2)^3$										
stack	N	$(n^1,l^1)\times(n^2,l^2)\times(n^3,l^3)$	$n_{\square\square}$	$n_{\begin{smallmatrix}\square\\\square\end{smallmatrix}}$	b	b'	c	c'	2	3	4
a	8	$(1,-1)\times(1,0)\times(1,1)$	0	0	3	0	0	-3	-1	0	1
b	4	$(-1,4)\times(0,1)\times(-1,1)$	3	-3	—	—	-7	0	0	1	0
c	4	$(-2,1)\times(-1,1)\times(1,1)$	-2	-6	—	—	—	—	-1	-2	2
2	2	$(1,0)\times(0,-1)\times(0,2)$	$x_A=\frac{1}{9}x_B=\frac{1}{4}x_C=\frac{1}{9}x_D$								
3	2	$(0,-1)\times(1,0)\times(0,2)$	$\beta_2^g=-3,\ \beta_3^g=-3,\ \beta_4^g=-2$								
4	2	$(0,-1)\times(0,1)\times(2,0)$	$\chi_1=\frac{1}{2},\ \chi_2=\frac{2}{9},\ \chi_3=1$								

Table 9. D6-brane configurations and intersection numbers of Model 2, and its MSSM gauge coupling relation is $g_a^2=\frac{4}{9}g_b^2=\frac{17}{9}g_c^2=\frac{85}{61}(\frac{5}{3}g_Y^2)=\frac{32\pi e^{\phi^4}}{15}$.

JHEP03(2023)210

Model 3	$\mathrm{U}(4)\times\mathrm{U}(2)_L\times\mathrm{U}(2)_R\times\mathrm{USp}(2)^2$									
stack	N	$(n^1,l^1)\times(n^2,l^2)\times(n^3,l^3)$	$n_{\square\square}$	$n_{\begin{smallmatrix}\square\\\square\end{smallmatrix}}$	b	b'	c	c'	1	4
a	8	$(-1,-1)\times(1,1)\times(1,1)$	0	-4	0	3	0	-3	1	-1
b	4	$(-5,2)\times(-1,0)\times(1,1)$	-3	3	—	—	0	1	0	5
c	4	$(-2,-1)\times(0,1)\times(1,1)$	1	-1	—	—	—	—	1	0
1	2	$(1,0)\times(1,0)\times(2,0)$	$x_A=\frac{14}{5}x_B=2x_C=7x_D$							
4	2	$(0,-1)\times(0,1)\times(2,0)$	$\beta_1^g=-3,\ \beta_4^g=1$							
			$\chi_1=\sqrt{5},\ \chi_2=\frac{7}{\sqrt{5}},\ \chi_3=\frac{4}{\sqrt{5}}$							

Table 10. D6-brane configurations and intersection numbers of Model 3, and its gauge coupling relation is $g_a^2=\frac{5}{6}g_b^2=\frac{7}{6}g_c^2=\frac{35}{32}(\frac{5}{3}g_Y^2)=\frac{8}{27}5^{3/4}\sqrt{7}\pi e^{\phi^4}$.

Model 4	$\mathrm{U}(4)\times\mathrm{U}(2)_L\times\mathrm{U}(2)_R\times\mathrm{USp}(4)$								
stack	N	$(n^1,l^1)\times(n^2,l^2)\times(n^3,l^3)$	$n_{\square\square}$	$n_{\begin{smallmatrix}\square\\\square\end{smallmatrix}}$	b	b'	c	c'	4
a	8	$(2,1)\times(1,0)\times(1,-1)$	1	-1	3	0	0	-3	-2
b	4	$(1,0)\times(1,-3)\times(1,1)$	2	-2	—	—	-4	0	1
c	4	$(-1,2)\times(-1,1)\times(-1,1)$	2	6	—	—	—	—	1
4	4	$(0,-1)\times(0,1)\times(2,0)$	$x_A=\frac{4}{3}x_B=8x_C=\frac{8}{3}x_D$						
			$\beta_4^g=0$						
			$\chi_1=4,\ \chi_2=\frac{2}{3},\ \chi_3=4$						

Table 11. D6-brane configurations and intersection numbers of Model 4, and its MSSM gauge coupling relation is $g_a^2=\frac{1}{2}g_b^2=\frac{13}{6}g_c^2=\frac{65}{44}(\frac{5}{3}g_Y^2)=\frac{16}{5}\sqrt{\frac{2}{3}}\pi e^{\phi^4}$.

Model 5	$\mathrm{U}(4)\times\mathrm{U}(2)_L\times\mathrm{U}(2)_R\times\mathrm{USp}(4)$								
stack	N	$(n^1,l^1)\times(n^2,l^2)\times(n^3,l^3)$	$n_{\square\square}$	$n_{\begin{smallmatrix}\square\\\square\end{smallmatrix}}$	b	b'	c	c'	3
a	8	$(-1,1)\times(-1,0)\times(1,1)$	0	0	3	0	0	-3	0
b	4	$(-1,4)\times(0,1)\times(-1,1)$	3	-3	—	—	-8	0	1
c	4	$(1,0)\times(2,-3)\times(1,1)$	1	-1	—	—	—	—	-3
3	4	$(0,-1)\times(1,0)\times(0,2)$	$x_A=\frac{1}{6}x_B=\frac{1}{4}x_C=\frac{1}{6}x_D$						
			$\beta_3^g=-2$						
			$\chi_1=\frac{1}{2},\ \chi_2=\frac{1}{3},\ \chi_3=1$						

Table 12. D6-brane configurations and intersection numbers of Model 5, and its MSSM gauge coupling relation is $g_a^2=\frac{2}{3}g_b^2=2g_c^2=\frac{10}{7}(\frac{5}{3}g_Y^2)=\frac{16}{5}\sqrt{\frac{2}{3}}\pi e^{\phi^4}$.

JHEP03(2023)210

Model 6	$\mathrm{U}(4)\times\mathrm{U}(2)_L\times\mathrm{U}(2)_R\times\mathrm{USp}(2)$								
stack	N	$(n^1,l^1)\times(n^2,l^2)\times(n^3,l^3)$	$n_{\square\!\square}$	$n_{\begin{smallmatrix}\square\\\square\end{smallmatrix}}$	b	b'	c	c'	3
a	8	$(1,-1)\times(1,0)\times(1,1)$	0	0	3	0	0	-3	0
b	4	$(-2,5)\times(0,1)\times(-1,1)$	3	-3	—	—	-8	0	2
c	4	$(-2,1)\times(-1,1)\times(1,1)$	-2	-6	—	—	—	—	-2
3	2	$(0,-1)\times(1,0)\times(0,2)$	$x_A=\frac{1}{6}x_B=\frac{2}{5}x_C=\frac{1}{6}x_D$ $\beta_3^g=-2$ $\chi_1=\sqrt{\frac{2}{5}}$, $\chi_2=\frac{\sqrt{\frac{5}{2}}}{6}$, $\chi_3=2\sqrt{\frac{2}{5}}$						

Table 13. D6-brane configurations and intersection numbers of Model 6, and its MSSM gauge coupling relation is $g_a^2=\frac{5}{6}g_b^2=\frac{11}{6}g_c^2=\frac{11}{8}(\frac{5}{3}g_Y^2)=\frac{8\sqrt[4]{2}5^{3/4}\pi e^{\phi^4}}{7\sqrt{3}}$.

Model 7	$\mathrm{U}(4)\times\mathrm{U}(2)_L\times\mathrm{U}(2)_R\times\mathrm{USp}(4)^2$									
stack	N	$(n^1,l^1)\times(n^2,l^2)\times(n^3,l^3)$	$n_{\square\!\square}$	$n_{\begin{smallmatrix}\square\\\square\end{smallmatrix}}$	b	b'	c	c'	2	4
a	8	$(1,1)\times(1,0)\times(1,-1)$	0	0	3	0	0	-3	1	-1
b	4	$(1,0)\times(1,-3)\times(1,1)$	2	-2	—	—	-4	0	0	1
c	4	$(1,2)\times(-1,1)\times(-1,1)$	-2	-6	—	—	—	—	2	-1
2	4	$(1,0)\times(0,-1)\times(0,2)$	$x_A=\frac{1}{3}x_B=x_C=\frac{1}{3}x_D$ $\beta_2^g=-2$, $\beta_4^g=-2$ $\chi_1=1$, $\chi_2=\frac{1}{3}$, $\chi_3=2$							
4	4	$(0,-1)\times(0,1)\times(2,0)$								

Table 14. D6-brane configurations and intersection numbers of Model 7, and its MSSM gauge coupling relation is $g_a^2=g_b^2=\frac{5}{3}g_c^2=\frac{25}{19}(\frac{5}{3}g_Y^2)=4\sqrt{\frac{2}{3}}\pi e^{\phi^4}$.

Model 8	$\mathrm{U}(4)\times\mathrm{U}(2)_L\times\mathrm{U}(2)_R\times\mathrm{USp}(2)^3$										
stack	N	$(n^1,l^1)\times(n^2,l^2)\times(n^3,l^3)$	$n_{\square\!\square}$	$n_{\begin{smallmatrix}\square\\\square\end{smallmatrix}}$	b	b'	c	c'	1	2	4
a	8	$(1,1)\times(1,0)\times(1,-1)$	0	0	3	0	0	-3	0	1	-1
b	4	$(-1,0)\times(-1,3)\times(1,1)$	2	-2	—	—	-3	0	0	0	1
c	4	$(0,1)\times(-2,3)\times(-1,1)$	1	-1	—	—	—	—	-3	2	0
1	2	$(1,0)\times(1,0)\times(2,0)$	$x_A=\frac{2}{3}x_B=2x_C=\frac{2}{3}x_D$ $\beta_1^g=-3$, $\beta_2^g=-2$, $\beta_4^g=-3$ $\chi_1=\sqrt{2}$, $\chi_2=\frac{\sqrt{2}}{3}$, $\chi_3=2\sqrt{2}$								
2	2	$(1,0)\times(0,-1)\times(0,2)$									
4	2	$(0,-1)\times(0,1)\times(2,0)$									

Table 15. D6-brane configurations and intersection numbers of Model 8, and its MSSM gauge coupling relation is $g_a^2=g_b^2=2g_c^2=\frac{10}{7}(\frac{5}{3}g_Y^2)=\frac{16\sqrt[4]{2}\pi e^{\phi^4}}{3\sqrt{3}}$.

JHEP03(2023)210

Model 9	$\mathrm{U}(4)\times\mathrm{U}(2)_L\times\mathrm{U}(2)_R\times\mathrm{USp}(2)^2$									
stack	N	$(n^1,l^1)\times(n^2,l^2)\times(n^3,l^3)$	$n_{\square\square}$	$n_{\begin{smallmatrix}\square\\\square\end{smallmatrix}}$	b	b'	c	c'	1	4
a	8	$(1,-1)\times(-1,1)\times(1,-1)$	0	4	3	0	0	-3	-1	1
b	4	$(1,-4)\times(1,0)\times(1,1)$	3	-3	—	—	-7	0	0	1
c	4	$(-2,1)\times(2,1)\times(-1,1)$	-3	-13	—	—	—	—	-1	-4
1	2	$(1,0)\times(1,0)\times(2,0)$	$x_A=28x_B=\frac{28}{23}x_C=7x_D$							
4	2	$(0,-1)\times(0,1)\times(2,0)$	$\beta_1^g=-3,\ \beta_4^g=1$							
			$\chi_1=\sqrt{\frac{7}{23}},\ \chi_2=\sqrt{161},\ \chi_3=8\sqrt{\frac{7}{23}}$							

Table 16. D6-brane configurations and intersection numbers of Model 9, and its MSSM gauge coupling relation is $g_a^2=\frac{1}{6}g_b^2=\frac{11}{6}g_c^2=\frac{11}{8}(\frac{5}{3}g_Y^2)=\frac{8}{405}161^{3/4}\sqrt{2}\pi e^{\phi^4}$.

Model 10	$\mathrm{U}(4)\times\mathrm{U}(2)_L\times\mathrm{U}(2)_R\times\mathrm{USp}(2)^2\times\mathrm{USp}(4)$									
stack	N	$(n^1,l^1)\times(n^2,l^2)\times(n^3,l^3)$	$n_{\square\square}$	$n_{\begin{smallmatrix}\square\\\square\end{smallmatrix}}$	b	b'	c	c'	1	3	4
a	8	$(-1,-1)\times(1,1)\times(1,1)$	0	-4	0	3	0	-3	1	-1	-1
b	4	$(-4,1)\times(-1,0)\times(1,1)$	-3	3	—	—	0	2	0	0	4
c	4	$(-2,-1)\times(0,1)\times(1,1)$	1	-1	—	—	—	—	1	-2	0
1	4	$(1,0)\times(1,0)\times(2,0)$	$x_A=\frac{5}{2}x_B=2x_C=10x_D$								
3	2	$(0,-1)\times(1,0)\times(0,2)$	$\beta_1^g=-3,\ \beta_3^g=-2,\ \beta_4^g=0$								
4	2	$(0,-1)\times(0,1)\times(2,0)$	$\chi_1=2\sqrt{2},\ \chi_2=\frac{5}{\sqrt{2}},\ \chi_3=\sqrt{2}$								

Table 17. D6-brane configurations and intersection numbers of Model 10, and its MSSM gauge coupling relation is $g_a^2=\frac{4}{9}g_b^2=\frac{10}{9}g_c^2=\frac{50}{47}(\frac{5}{3}g_Y^2)=\frac{16}{27}2^{3/4}\sqrt{5}\pi e^{\phi^4}$.

Model 11	$\mathrm{U}(4)\times\mathrm{U}(2)_L\times\mathrm{U}(2)_R\times\mathrm{USp}(2)\times\mathrm{USp}(4)$									
stack	N	$(n^1,l^1)\times(n^2,l^2)\times(n^3,l^3)$	$n_{\square\square}$	$n_{\begin{smallmatrix}\square\\\square\end{smallmatrix}}$	b	b'	c	c'	1	3
a	8	$(-1,1)\times(-1,0)\times(1,1)$	0	0	3	0	0	-3	0	0
b	4	$(-1,4)\times(0,1)\times(-1,1)$	3	-3	—	—	-4	0	-4	1
c	4	$(1,0)\times(1,-3)\times(1,1)$	2	-2	—	—	—	—	0	-3
1	2	$(1,0)\times(1,0)\times(2,0)$	$x_A=\frac{1}{12}x_B=\frac{1}{4}x_C=\frac{1}{12}x_D$							
3	4	$(0,-1)\times(1,0)\times(0,2)$	$\beta_1^g=-2,\ \beta_3^g=-2$							
			$\chi_1=\frac{1}{2},\ \chi_2=\frac{1}{6},\ \chi_3=1$							

Table 18. D6-brane configurations and intersection numbers of Model 11, and its MSSM gauge coupling relation is $g_a^2=\frac{1}{3}g_b^2=g_c^2=(\frac{5}{3}g_Y^2)=\frac{16\pi e^{\phi^4}}{5\sqrt{3}}$.

JHEP03(2023)210

Model 12	$\mathrm{U}(4)\times\mathrm{U}(2)_L\times\mathrm{U}(2)_R\times\mathrm{USp}(2)\times\mathrm{USp}(4)$									
stack	N	$(n^1,l^1)\times(n^2,l^2)\times(n^3,l^3)$	$n_{\square\square}$	$n_{\begin{smallmatrix}\square\\\square\end{smallmatrix}}$	b	b'	c	c'	1	4
a	8	$(-1,-1)\times(2,1)\times(1,1)$	0	-8	0	3	0	-3	1	-2
b	4	$(4,-1)\times(1,0)\times(1,1)$	-3	3	—	—	0	2	0	4
c	4	$(-2,-1)\times(-1,1)\times(1,1)$	2	6	—	—	—	—	1	2
1	4	$(1,0)\times(1,0)\times(2,0)$	$x_A=\frac{13}{2}x_B=\frac{13}{8}x_C=26x_D$							
4	2	$(0,-1)\times(0,1)\times(2,0)$	$\beta_1^g=-3,\ \beta_4^g=4$							
			$\chi_1=\sqrt{\frac{13}{2}},\ \chi_2=2\sqrt{26},\ \chi_3=\frac{\sqrt{\frac{13}{2}}}{2}$							

Table 19. D6-brane configurations and intersection numbers of Model 12, and its MSSM gauge coupling relation is $g_a^2=\frac{1}{6}g_b^2=\frac{7}{6}g_c^2=\frac{35}{32}(\frac{5}{3}g_Y^2)=\frac{16}{135}26^{3/4}\pi e^{\phi^4}$.

Model 13	$\mathrm{U}(4)\times\mathrm{U}(2)_L\times\mathrm{U}(2)_R\times\mathrm{USp}(2)^2$									
stack	N	$(n^1,l^1)\times(n^2,l^2)\times(n^3,l^3)$	$n_{\square\square}$	$n_{\begin{smallmatrix}\square\\\square\end{smallmatrix}}$	b	b'	c	c'	1	4
a	8	$(-1,-1)\times(1,1)\times(1,1)$	0	-4	6	-3	0	-3	1	-1
b	4	$(-1,2)\times(-1,0)\times(5,1)$	9	-9	—	—	-10	-9	0	1
c	4	$(-2,-1)\times(0,1)\times(1,1)$	1	-1	—	—	—	—	1	0
1	2	$(1,0)\times(1,0)\times(2,0)$	$x_A=22x_B=2x_C=\frac{11}{5}x_D$							
4	2	$(0,-1)\times(0,1)\times(2,0)$	$\beta_1^g=-3,\ \beta_4^g=-3$							
			$\chi_1=\frac{1}{\sqrt{5}},\ \chi_2=\frac{11}{\sqrt{5}},\ \chi_3=4\sqrt{5}$							

Table 20. D6-brane configurations and intersection numbers of Model 13, and its MSSM gauge coupling relation is $g_a^2=\frac{5}{14}g_b^2=\frac{11}{6}g_c^2=\frac{11}{8}(\frac{5}{3}g_Y^2)=\frac{8}{63}5^{3/4}\sqrt{11}\pi e^{\phi^4}$.

Model 14	$\mathrm{U}(4)\times\mathrm{U}(2)_L\times\mathrm{U}(2)_R\times\mathrm{USp}(2)$								
stack	N	$(n^1,l^1)\times(n^2,l^2)\times(n^3,l^3)$	$n_{\square\square}$	$n_{\begin{smallmatrix}\square\\\square\end{smallmatrix}}$	b	b'	c	c'	3
a	8	$(1,-1)\times(1,0)\times(1,1)$	0	0	-3	6	0	-3	0
b	4	$(-2,1)\times(0,1)\times(-5,1)$	-9	9	—	—	0	8	10
c	4	$(-2,1)\times(-1,1)\times(1,1)$	-2	-6	—	—	—	—	-2
3	2	$(0,-1)\times(1,0)\times(0,2)$	$x_A=\frac{5}{6}x_B=10x_C=\frac{5}{6}x_D$						
			$\beta_3^g=6$						
			$\chi_1=\sqrt{10},\ \chi_2=\frac{\sqrt{\frac{5}{2}}}{6},\ \chi_3=2\sqrt{10}$						

Table 21. D6-brane configurations and intersection numbers of Model 14, and its MSSM gauge coupling relation is $g_a^2=\frac{35}{66}g_b^2=\frac{7}{6}g_c^2=\frac{35}{32}(\frac{5}{3}g_Y^2)=\frac{8\sqrt[4]{2}5^{3/4}\pi e^{\phi^4}}{11\sqrt{3}}$.

JHEP03(2023)210

Model 15	$\mathrm{U}(4)\times\mathrm{U}(2)_L\times\mathrm{U}(2)_R\times\mathrm{USp}(2)^2$									
stack	N	$(n^1,l^1)\times(n^2,l^2)\times(n^3,l^3)$	$n_{\square\square}$	$n_{\begin{smallmatrix}\square\\\square\end{smallmatrix}}$	b	b'	c	c'	1	4
a	8	$(1,-1)\times(-1,1)\times(1,-1)$	0	4	0	3	0	-3	-1	1
b	4	$(0,1)\times(-2,1)\times(-1,1)$	-1	1	—	—	0	-1	-1	0
c	4	$(-1,0)\times(5,2)\times(-1,1)$	3	-3	—	—	—	—	0	-5
1	2	$(1,0)\times(1,0)\times(2,0)$	$x_A=2x_B=\frac{14}{5}x_C=7x_D$							
4	2	$(0,-1)\times(0,1)\times(2,0)$	$\beta_1^g=-3,\ \beta_4^g=1$							
			$\chi_1=\frac{7}{\sqrt{5}},\ \chi_2=\sqrt{5},\ \chi_3=\frac{4}{\sqrt{5}}$							

Table 22. D6-brane configurations and intersection numbers of Model 15, and its gauge coupling relation is $g_a^2=\frac{7}{6}g_b^2=\frac{5}{6}g_c^2=\frac{25}{28}(\frac{5}{3}g_Y^2)=\frac{8}{27}5^{3/4}\sqrt{7}\pi e^{\phi^4}$.

Model 16	$\mathrm{U}(4)\times\mathrm{U}(2)_L\times\mathrm{U}(2)_R\times\mathrm{USp}(2)^2$									
stack	N	$(n^1,l^1)\times(n^2,l^2)\times(n^3,l^3)$	$n_{\square\square}$	$n_{\begin{smallmatrix}\square\\\square\end{smallmatrix}}$	b	b'	c	c'	2	4
a	8	$(1,1)\times(1,0)\times(1,-1)$	0	0	2	1	0	-3	1	-1
b	4	$(-1,0)\times(-2,1)\times(1,3)$	-5	5	—	—	8	8	0	6
c	4	$(0,1)\times(-2,3)\times(-1,1)$	1	-1	—	—	—	—	2	0
2	2	$(1,0)\times(0,-1)\times(0,2)$	$x_A=\frac{2}{3}x_B=\frac{1}{9}x_C=\frac{2}{3}x_D$							
4	2	$(0,-1)\times(0,1)\times(2,0)$	$\beta_2^g=-2,\ \beta_4^g=2$							
			$\chi_1=\frac{1}{3},\ \chi_2=2,\ \chi_3=\frac{2}{3}$							

Table 23. D6-brane configurations and intersection numbers of Model 16, and its MSSM gauge coupling relation is $g_a^2=\frac{18}{5}g_b^2=2g_c^2=\frac{10}{7}(\frac{5}{3}g_Y^2)=\frac{24\pi e^{\phi^4}}{5}$.

Model 17	$\mathrm{U}(4)\times\mathrm{U}(2)_L\times\mathrm{U}(2)_R\times\mathrm{USp}(2)^2$									
stack	N	$(n^1,l^1)\times(n^2,l^2)\times(n^3,l^3)$	$n_{\square\square}$	$n_{\begin{smallmatrix}\square\\\square\end{smallmatrix}}$	b	b'	c	c'	2	4
a	8	$(1,1)\times(1,0)\times(1,-1)$	0	0	3	0	0	-3	1	-1
b	4	$(-1,0)\times(-2,3)\times(1,1)$	1	-1	—	—	0	0	0	2
c	4	$(0,1)\times(-2,3)\times(-1,1)$	1	-1	—	—	—	—	2	0
2	2	$(1,0)\times(0,-1)\times(0,2)$	$x_A=\frac{2}{3}x_B=x_C=\frac{2}{3}x_D$							
4	2	$(0,-1)\times(0,1)\times(2,0)$	$\beta_2^g=-2,\ \beta_4^g=-2$							
			$\chi_1=1,\ \chi_2=\frac{2}{3},\ \chi_3=2$							

Table 24. D6-brane configurations and intersection numbers of Model 17, and its MSSM gauge coupling relation is $g_a^2=2g_b^2=2g_c^2=\frac{10}{7}(\frac{5}{3}g_Y^2)=\frac{8\pi e^{\phi^4}}{\sqrt{3}}$.

JHEP03(2023)210

Model 18	$\mathrm{U}(4)\times\mathrm{U}(2)_L\times\mathrm{U}(2)_R\times\mathrm{USp}(2)^2$									
stack	N	$(n^1,l^1)\times(n^2,l^2)\times(n^3,l^3)$	$n_{\square\square}$	$n_{\begin{smallmatrix}\square\\\square\end{smallmatrix}}$	b	b'	c	c'	1	4
a	8	$(-1,-1)\times(1,1)\times(1,1)$	0	-4	3	0	0	-3	1	-1
b	4	$(-2,1)\times(2,1)\times(-1,1)$	-3	-13	—	—	7	0	-1	-4
c	4	$(1,-4)\times(1,0)\times(1,1)$	3	-3	—	—	—	—	0	1
1	2	$(1,0)\times(1,0)\times(2,0)$	$x_A=28x_B=\frac{28}{23}x_C=7x_D$							
4	2	$(0,-1)\times(0,1)\times(2,0)$	$\beta_1^g=-3,\ \beta_4^g=1$							
			$\chi_1=\sqrt{\frac{7}{23}},\ \chi_2=\sqrt{161},\ \chi_3=8\sqrt{\frac{7}{23}}$							

Table 25. D6-brane configurations and intersection numbers of Model 18, and its MSSM gauge coupling relation is $g_a^2=\frac{11}{6}g_b^2=\frac{1}{6}g_c^2=\frac{1}{4}(\frac{5}{3}g_Y^2)=\frac{8}{405}\sqrt{2}161^{3/4}\pi e^{\phi^4}$.

Model 19	$\mathrm{U}(4)\times\mathrm{U}(2)_L\times\mathrm{U}(2)_R\times\mathrm{USp}(4)^2$									
stack	N	$(n^1,l^1)\times(n^2,l^2)\times(n^3,l^3)$	$n_{\square\square}$	$n_{\begin{smallmatrix}\square\\\square\end{smallmatrix}}$	b	b'	c	c'	2	4
a	8	$(1,1)\times(1,0)\times(1,-1)$	0	0	3	0	0	-3	1	-1
b	4	$(-2,1)\times(-1,1)\times(1,1)$	-2	-6	—	—	4	0	-1	2
c	4	$(0,1)\times(-1,3)\times(-1,1)$	2	-2	—	—	—	—	1	0
2	4	$(1,0)\times(0,-1)\times(0,2)$	$x_A=\frac{1}{3}x_B=x_C=\frac{1}{3}x_D$							
4	4	$(0,-1)\times(0,1)\times(2,0)$	$\beta_2^g=-2,\ \beta_4^g=-2$							
			$\chi_1=1,\ \chi_2=\frac{1}{3},\ \chi_3=2$							

Table 26. D6-brane configurations and intersection numbers of Model 19, and its MSSM gauge coupling relation is $g_a^2=\frac{5}{3}g_b^2=g_c^2=(\frac{5}{3}g_Y^2)=4\sqrt{\frac{2}{3}}\pi e^{\phi^4}$.

Model 20	$\mathrm{U}(4)\times\mathrm{U}(2)_L\times\mathrm{U}(2)_R\times\mathrm{USp}(2)^3$										
stack	N	$(n^1,l^1)\times(n^2,l^2)\times(n^3,l^3)$	$n_{\square\square}$	$n_{\begin{smallmatrix}\square\\\square\end{smallmatrix}}$	b	b'	c	c'	2	3	4
a	8	$(1,1)\times(1,0)\times(1,-1)$	0	0	3	0	0	-3	1	0	-1
b	4	$(-1,0)\times(-2,3)\times(1,1)$	1	-1	—	—	3	0	0	-3	2
c	4	$(0,1)\times(-1,3)\times(-1,1)$	2	-2	—	—	—	—	1	0	0
2	2	$(1,0)\times(0,-1)\times(0,2)$	$x_A=\frac{1}{3}x_B=\frac{1}{2}x_C=\frac{1}{3}x_D$								
3	2	$(0,-1)\times(1,0)\times(0,2)$	$\beta_2^g=-3,\ \beta_3^g=-3,\ \beta_4^g=-2$								
4	2	$(0,-1)\times(0,1)\times(2,0)$	$\chi_1=\frac{1}{\sqrt{2}},\ \chi_2=\frac{\sqrt{2}}{3},\ \chi_3=\sqrt{2}$								

Table 27. D6-brane configurations and intersection numbers of Model 20, and its MSSM gauge coupling relation is $g_a^2=2g_b^2=g_c^2=(\frac{5}{3}g_Y^2)=\frac{16\sqrt[4]{2}\pi e^{\phi^4}}{3\sqrt{3}}$.

JHEP03(2023)210

Model 21	$\mathrm{U}(4)\times\mathrm{U}(2)_L\times\mathrm{U}(2)_R\times\mathrm{USp}(2)^3$										
stack	N	$(n^1,l^1)\times(n^2,l^2)\times(n^3,l^3)$	$n_{\square\square}$	$n_{\begin{smallmatrix}\square\\\square\end{smallmatrix}}$	b	b'	c	c'	2	3	4
a	8	$(1,1)\times(1,0)\times(1,-1)$	0	0	2	1	0	-3	1	0	-1
b	4	$(-1,0)\times(-2,1)\times(1,3)$	-5	5	—	—	10	7	0	-1	6
c	4	$(0,1)\times(-1,3)\times(-1,1)$	2	-2	—	—	—	—	1	0	0
2	2	$(1,0)\times(0,-1)\times(0,2)$	$x_A=\frac{1}{3}x_B=\frac{1}{18}x_C=\frac{1}{3}x_D$								
3	2	$(0,-1)\times(1,0)\times(0,2)$	$\beta_2^g=-3,\ \beta_3^g=-5,\ \beta_4^g=2$								
4	2	$(0,-1)\times(0,1)\times(2,0)$	$\chi_1=\frac{1}{3\sqrt{2}},\ \chi_2=\sqrt{2},\ \chi_3=\frac{\sqrt{2}}{3}$								

Table 28. D6-brane configurations and intersection numbers of Model 21, and its MSSM gauge coupling relation is $g_a^2=\frac{54}{19}g_b^2=g_c^2=(\frac{5}{3}g_Y^2)=\frac{48}{19}\sqrt[4]{2}\pi e^{\phi^4}$.

Model 22	$\mathrm{U}(4)\times\mathrm{U}(2)_L\times\mathrm{U}(2)_R\times\mathrm{USp}(2)^4$											
stack	N	$(n^1,l^1)\times(n^2,l^2)\times(n^3,l^3)$	$n_{\square\square}$	$n_{\begin{smallmatrix}\square\\\square\end{smallmatrix}}$	b	b'	c	c'	1	2	3	4
a	8	$(1,1)\times(1,0)\times(1,-1)$	0	0	2	1	0	-3	0	1	0	-1
b	4	$(-1,0)\times(-1,1)\times(1,3)$	-2	2	—	—	4	4	0	0	-1	3
c	4	$(0,1)\times(-1,3)\times(-1,1)$	2	-2	—	—	—	—	-3	1	0	0
1	2	$(1,0)\times(1,0)\times(2,0)$	$x_A=\frac{1}{3}x_B=\frac{1}{9}x_C=\frac{1}{3}x_D$									
2	2	$(1,0)\times(0,-1)\times(0,2)$	$\beta_1^g=-3,\ \beta_2^g=-3,\ \beta_3^g=-5,\ \beta_4^g=-1$									
3	2	$(0,-1)\times(1,0)\times(0,2)$	$\chi_1=\frac{1}{3},\ \chi_2=1,\ \chi_3=\frac{2}{3}$									
4	2	$(0,-1)\times(0,1)\times(2,0)$										

Table 29. D6-brane configurations and intersection numbers of Model 22, and its MSSM gauge coupling relation is $g_a^2=\frac{9}{5}g_b^2=g_c^2=(\frac{5}{3}g_Y^2)=\frac{12}{5}\sqrt{2}\pi e^{\phi^4}$.

Model 23	$\mathrm{U}(4)\times\mathrm{U}(2)_L\times\mathrm{U}(2)_R\times\mathrm{USp}(4)$								
stack	N	$(n^1,l^1)\times(n^2,l^2)\times(n^3,l^3)$	$n_{\square\square}$	$n_{\begin{smallmatrix}\square\\\square\end{smallmatrix}}$	b	b'	c	c'	4
a	8	$(-2,1)\times(-1,0)\times(1,1)$	-1	1	3	0	0	-3	2
b	4	$(-1,2)\times(-1,1)\times(-1,1)$	2	6	—	—	4	0	1
c	4	$(1,0)\times(1,-3)\times(1,1)$	2	-2	—	—	—	—	1
4	4	$(0,-1)\times(0,1)\times(2,0)$	$x_A=\frac{4}{3}x_B=8x_C=\frac{8}{3}x_D$ $\beta_4^g=0$ $\chi_1=4,\ \chi_2=\frac{2}{3},\ \chi_3=4$						

Table 30. D6-brane configurations and intersection numbers of Model 23, and its MSSM gauge coupling relation is $g_a^2=\frac{13}{6}g_b^2=\frac{1}{2}g_c^2=\frac{5}{8}(\frac{5}{3}g_Y^2)=\frac{16}{5}\sqrt{\frac{2}{3}}\pi e^{\phi^4}$.

JHEP03(2023)210

Model 24	$\mathrm{U}(4)\times\mathrm{U}(2)_L\times\mathrm{U}(2)_R\times\mathrm{USp}(4)$								
stack	N	$(n^1,l^1)\times(n^2,l^2)\times(n^3,l^3)$	$n_{\square\square}$	$n_{\begin{smallmatrix}\square\\\square\end{smallmatrix}}$	b	b'	c	c'	3
a	8	$(1,1)\times(-1,0)\times(-1,1)$	0	0	3	0	0	-3	0
b	4	$(1,0)\times(2,-3)\times(1,1)$	1	-1	—	—	8	0	-3
c	4	$(-1,4)\times(0,1)\times(-1,1)$	3	-3	—	—	—	—	1
3	4	$(0,-1)\times(1,0)\times(0,2)$	$x_A=\frac{1}{6}x_B=\frac{1}{4}x_C=\frac{1}{6}x_D$ $\beta_3^g=-2$ $\chi_1=\frac{1}{2},\ \chi_2=\frac{1}{3},\ \chi_3=1$						

Table 31. D6-brane configurations and intersection numbers of Model 24, and its MSSM gauge coupling relation is $g_a^2=2g_b^2=\frac{2}{3}g_c^2=\frac{10}{13}(\frac{5}{3}g_Y^2)=\frac{16}{5}\sqrt{\frac{2}{3}}\pi e^{\phi^4}$.

Model 25	$\mathrm{U}(4)\times\mathrm{U}(2)_L\times\mathrm{U}(2)_R\times\mathrm{USp}(2)^3$										
stack	N	$(n^1,l^1)\times(n^2,l^2)\times(n^3,l^3)$	$n_{\square\square}$	$n_{\begin{smallmatrix}\square\\\square\end{smallmatrix}}$	b	b'	c	c'	2	3	4
a	8	$(1,1)\times(1,0)\times(1,-1)$	0	0	3	0	0	-3	1	0	-1
b	4	$(2,-1)\times(1,-1)\times(1,1)$	-2	-6	—	—	7	0	-1	-2	2
c	4	$(-1,4)\times(0,1)\times(-1,1)$	3	-3	—	—	—	—	0	1	0
2	2	$(1,0)\times(0,-1)\times(0,2)$	$x_A=\frac{1}{9}x_B=\frac{1}{4}x_C=\frac{1}{9}x_D$ $\beta_2^g=-3,\ \beta_3^g=-3,\ \beta_4^g=-2$ $\chi_1=\frac{1}{2},\ \chi_2=\frac{2}{9},\ \chi_3=1$								
3	2	$(0,-1)\times(1,0)\times(0,2)$									
4	2	$(0,-1)\times(0,1)\times(2,0)$									

Table 32. D6-brane configurations and intersection numbers of Model 25, and its MSSM gauge coupling relation is $g_a^2=\frac{17}{9}g_b^2=\frac{4}{9}g_c^2=\frac{4}{7}(\frac{5}{3}g_Y^2)=\frac{32\pi e^{\phi^4}}{15}$.

Model 26	$\mathrm{U}(4)\times\mathrm{U}(2)_L\times\mathrm{U}(2)_R\times\mathrm{USp}(2)$								
stack	N	$(n^1,l^1)\times(n^2,l^2)\times(n^3,l^3)$	$n_{\square\square}$	$n_{\begin{smallmatrix}\square\\\square\end{smallmatrix}}$	b	b'	c	c'	3
a	8	$(1,1)\times(1,0)\times(1,-1)$	0	0	3	0	0	-3	0
b	4	$(2,-1)\times(1,-1)\times(1,1)$	-2	-6	—	—	8	0	-2
c	4	$(-2,5)\times(0,1)\times(-1,1)$	3	-3	—	—	—	—	2
3	2	$(0,-1)\times(1,0)\times(0,2)$	$x_A=\frac{1}{6}x_B=\frac{2}{5}x_C=\frac{1}{6}x_D$ $\beta_3^g=-2$ $\chi_1=\sqrt{\frac{2}{5}},\ \chi_2=\frac{\sqrt{\frac{5}{2}}}{6},\ \chi_3=2\sqrt{\frac{2}{5}}$						

Table 33. D6-brane configurations and intersection numbers of Model 26, and its MSSM gauge coupling relation is $g_a^2=\frac{11}{6}g_b^2=\frac{5}{6}g_c^2=\frac{25}{28}(\frac{5}{3}g_Y^2)=\frac{8\sqrt[4]{2}5^{3/4}\pi e^{\phi^4}}{7\sqrt{3}}$.

JHEP03(2023)210

Model 27	$\mathrm{U}(4)\times\mathrm{U}(2)_L\times\mathrm{U}(2)_R\times\mathrm{USp}(2)^2\times\mathrm{USp}(4)$										
stack	N	$(n^1,l^1)\times(n^2,l^2)\times(n^3,l^3)$	$n_{\square\square}$	$n_{\begin{smallmatrix}\square\\\square\end{smallmatrix}}$	b	b'	c	c'	1	2	4
a	8	$(1,-1)\times(-1,1)\times(1,-1)$	0	4	0	3	0	-3	-1	1	1
b	4	$(0,1)\times(-2,1)\times(-1,1)$	-1	1	—	—	0	-2	-1	2	0
c	4	$(-1,0)\times(4,1)\times(-1,1)$	3	-3	—	—	—	—	0	0	-4
1	4	$(1,0)\times(1,0)\times(2,0)$	$x_A=2x_B=\frac{5}{2}x_C=10x_D$								
2	2	$(1,0)\times(0,-1)\times(0,2)$	$\beta_1^g=-3,\ \beta_2^g=-2,\ \beta_4^g=0$								
4	2	$(0,-1)\times(0,1)\times(2,0)$	$\chi_1=\frac{5}{\sqrt{2}},\ \chi_2=2\sqrt{2},\ \chi_3=\sqrt{2}$								

Table 34. D6-brane configurations and intersection numbers of Model 27, and its MSSM gauge coupling relation is $g_a^2=\frac{10}{9}g_b^2=\frac{4}{9}g_c^2=\frac{4}{7}(\frac{5}{3}g_Y^2)=\frac{16}{27}2^{3/4}\sqrt{5}\pi e^{\phi^4}$.

Model 28	$\mathrm{U}(4)\times\mathrm{U}(2)_L\times\mathrm{U}(2)_R\times\mathrm{USp}(2)\times\mathrm{USp}(4)$									
stack	N	$(n^1,l^1)\times(n^2,l^2)\times(n^3,l^3)$	$n_{\square\square}$	$n_{\begin{smallmatrix}\square\\\square\end{smallmatrix}}$	b	b'	c	c'	1	3
a	8	$(1,1)\times(-1,0)\times(-1,1)$	0	0	3	0	0	-3	0	0
b	4	$(1,0)\times(1,-3)\times(1,1)$	2	-2	—	—	4	0	0	-3
c	4	$(-1,4)\times(0,1)\times(-1,1)$	3	-3	—	—	—	—	-4	1
1	2	$(1,0)\times(1,0)\times(2,0)$	$x_A=\frac{1}{12}x_B=\frac{1}{4}x_C=\frac{1}{12}x_D$							
3	4	$(0,-1)\times(1,0)\times(0,2)$	$\beta_1^g=-2,\ \beta_3^g=-2$							
			$\chi_1=\frac{1}{2},\ \chi_2=\frac{1}{6},\ \chi_3=1$							

Table 35. D6-brane configurations and intersection numbers of Model 28, and its MSSM gauge coupling relation is $g_a^2=g_b^2=\frac{1}{3}g_c^2=\frac{5}{11}(\frac{5}{3}g_Y^2)=\frac{16\pi e^{\phi^4}}{5\sqrt{3}}$.

Model 29	$\mathrm{U}(4)\times\mathrm{U}(2)_L\times\mathrm{U}(2)_R\times\mathrm{USp}(2)\times\mathrm{USp}(4)$									
stack	N	$(n^1,l^1)\times(n^2,l^2)\times(n^3,l^3)$	$n_{\square\square}$	$n_{\begin{smallmatrix}\square\\\square\end{smallmatrix}}$	b	b'	c	c'	1	4
a	8	$(1,-1)\times(-2,1)\times(1,-1)$	0	8	0	3	0	-3	-1	2
b	4	$(-2,1)\times(1,1)\times(-1,1)$	-2	-6	—	—	0	-2	-1	-2
c	4	$(-4,-1)\times(1,0)\times(-1,1)$	3	-3	—	—	—	—	0	-4
1	4	$(1,0)\times(1,0)\times(2,0)$	$x_A=\frac{13}{2}x_B=\frac{13}{8}x_C=26x_D$							
4	2	$(0,-1)\times(0,1)\times(2,0)$	$\beta_1^g=-3,\ \beta_4^g=4$							
			$\chi_1=\sqrt{\frac{13}{2}},\ \chi_2=2\sqrt{26},\ \chi_3=\frac{\sqrt{\frac{13}{2}}}{2}$							

Table 36. D6-brane configurations and intersection numbers of Model 29, and its MSSM gauge coupling relation is $g_a^2=\frac{7}{6}g_b^2=\frac{1}{6}g_c^2=\frac{1}{4}(\frac{5}{3}g_Y^2)=\frac{16}{135}26^{3/4}\pi e^{\phi^4}$.

JHEP03(2023)210

Model 30	$\mathrm{U}(4)\times\mathrm{U}(2)_L\times\mathrm{U}(2)_R\times\mathrm{USp}(2)^3$										
stack	N	$(n^1,l^1)\times(n^2,l^2)\times(n^3,l^3)$	$n_{\square\square}$	$n_{\begin{smallmatrix}\square\\\square\end{smallmatrix}}$	b	b'	c	c'	1	2	4
a	8	$(1,1)\times(1,0)\times(1,-1)$	0	0	2	1	0	-3	0	1	-1
b	4	$(-1,0)\times(-1,1)\times(1,3)$	-2	2	—	—	2	5	0	0	3
c	4	$(0,1)\times(-2,3)\times(-1,1)$	1	-1	—	—	—	—	-3	2	0
1	2	$(1,0)\times(1,0)\times(2,0)$	$x_A=\frac{2}{3}x_B=\frac{2}{9}x_C=\frac{2}{3}x_D$								
2	2	$(1,0)\times(0,-1)\times(0,2)$	$\beta_1^g=-3,\ \beta_2^g=-2,\ \beta_4^g=-1$								
4	2	$(0,-1)\times(0,1)\times(2,0)$	$\chi_1=\frac{\sqrt{2}}{3},\ \chi_2=\sqrt{2},\ \chi_3=\frac{2\sqrt{2}}{3}$								

Table 37. D6-brane configurations and intersection numbers of Model 30, and its MSSM gauge coupling relation is $g_a^2=\frac{27}{11}g_b^2=2g_c^2=\frac{10}{7}(\frac{5}{3}g_Y^2)=\frac{48}{11}\sqrt[4]{2}\pi e^{\phi^4}$.

Model 31	$\mathrm{U}(4)\times\mathrm{U}(2)_L\times\mathrm{U}(2)_R\times\mathrm{USp}(2)\times\mathrm{USp}(4)$									
stack	N	$(n^1,l^1)\times(n^2,l^2)\times(n^3,l^3)$	$n_{\square\square}$	$n_{\begin{smallmatrix}\square\\\square\end{smallmatrix}}$	b	b'	c	c'	1	3
a	8	$(1,1)\times(-1,0)\times(-1,1)$	0	0	2	1	0	-3	0	0
b	4	$(1,0)\times(1,-1)\times(1,3)$	-2	2	—	—	8	4	0	-1
c	4	$(-1,4)\times(0,1)\times(-1,1)$	3	-3	—	—	—	—	-4	1
1	2	$(1,0)\times(1,0)\times(2,0)$	$x_A=\frac{3}{4}x_B=\frac{1}{4}x_C=\frac{3}{4}x_D$							
3	4	$(0,-1)\times(1,0)\times(0,2)$	$\beta_1^g=-2,\ \beta_3^g=-4$							
			$\chi_1=\frac{1}{2},\ \chi_2=\frac{3}{2},\ \chi_3=1$							

Table 38. D6-brane configurations and intersection numbers of Model 31, and its MSSM gauge coupling relation is $g_a^2=\frac{13}{5}g_b^2=3g_c^2=\frac{5}{3}(\frac{5}{3}g_Y^2)=\frac{16}{5}\sqrt{3}\pi e^{\phi^4}$.

Model 32	$\mathrm{U}(4)\times\mathrm{U}(2)_L\times\mathrm{U}(2)_R\times\mathrm{USp}(4)$								
stack	N	$(n^1,l^1)\times(n^2,l^2)\times(n^3,l^3)$	$n_{\square\square}$	$n_{\begin{smallmatrix}\square\\\square\end{smallmatrix}}$	b	b'	c	c'	4
a	8	$(2,1)\times(1,0)\times(1,-1)$	1	-1	2	1	0	-3	-2
b	4	$(1,0)\times(1,-1)\times(1,3)$	-2	2	—	—	0	4	3
c	4	$(-1,2)\times(-1,1)\times(-1,1)$	2	6	—	—	—	—	1
4	4	$(0,-1)\times(0,1)\times(2,0)$	$x_A=2x_B=\frac{4}{3}x_C=4x_D$						
			$\beta_4^g=2$						
			$\chi_1=2\sqrt{\frac{2}{3}},\ \chi_2=\sqrt{6},\ \chi_3=2\sqrt{\frac{2}{3}}$						

Table 39. D6-brane configurations and intersection numbers of Model 32, and its MSSM gauge coupling relation is $g_a^2=\frac{21}{10}g_b^2=\frac{7}{2}g_c^2=\frac{7}{4}(\frac{5}{3}g_Y^2)=\frac{8}{5}6^{3/4}\pi e^{\phi^4}$.

JHEP03(2023)210

Model 33	$\mathrm{U}(4)\times\mathrm{U}(2)_L\times\mathrm{U}(2)_R\times\mathrm{USp}(4)$								
stack	N	$(n^1,l^1)\times(n^2,l^2)\times(n^3,l^3)$	$n_{\square\square}$	$n_{\begin{smallmatrix}\square\\\square\end{smallmatrix}}$	b	b'	c	c'	3
a	8	$(1,1)\times(-1,0)\times(-1,1)$	0	0	2	1	0	-3	0
b	4	$(1,0)\times(2,-1)\times(1,3)$	-5	5	—	—	16	8	-1
c	4	$(-1,4)\times(0,1)\times(-1,1)$	3	-3	—	—	—	—	1
3	4	$(0,-1)\times(1,0)\times(0,2)$	$x_A=\frac{3}{2}x_B=\frac{1}{4}x_C=\frac{3}{2}x_D$ $\beta_3^g=-4$ $\chi_1=\frac{1}{2},\ \chi_2=3,\ \chi_3=1$						

Table 40. D6-brane configurations and intersection numbers of Model 33, and its MSSM gauge coupling relation is $g_a^2=\frac{26}{5}g_b^2=6g_c^2=2(\frac{5}{3}g_Y^2)=\frac{16}{5}\sqrt{6}\pi e^{\phi^4}$.

JHEP03(2023)210

B The evolution for the gauge couplings

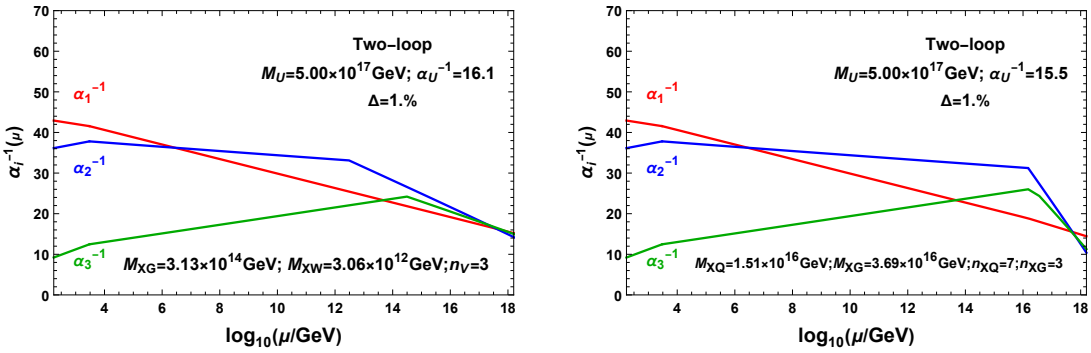

(a) (b)

Figure 11. Two-loop evolution of gauge couplings for the **Model 6** with vector-like particles. In the model, $k_Y = 1 \times \frac{11}{8}$ and $k_2 = \frac{5}{6}$. The string-scale gauge coupling relations can be achieved by adding $3(XG + XW)$ (a) and $7(XQ + \overline{XQ}) + 3XG$ (b).

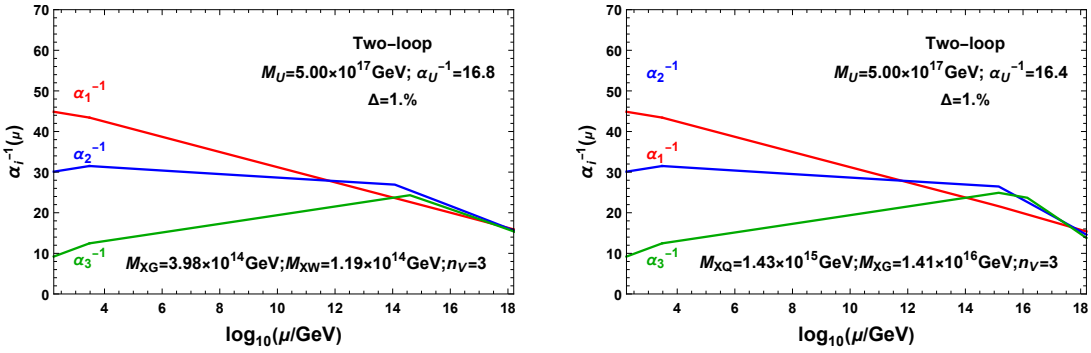

(a) (b)

Figure 12. Two-loop evolution of gauge couplings for the **Model 7** with vector-like particles. In the model, $k_Y = \frac{25}{19} \times \frac{5}{3}$ and $k_2 = 1$. The string-scale gauge coupling relations can be achieved by adding $3(XG + XW)$ (a) and $3(XQ + \overline{XQ}) + 3XG$ (b).

JHEP03(2023)210

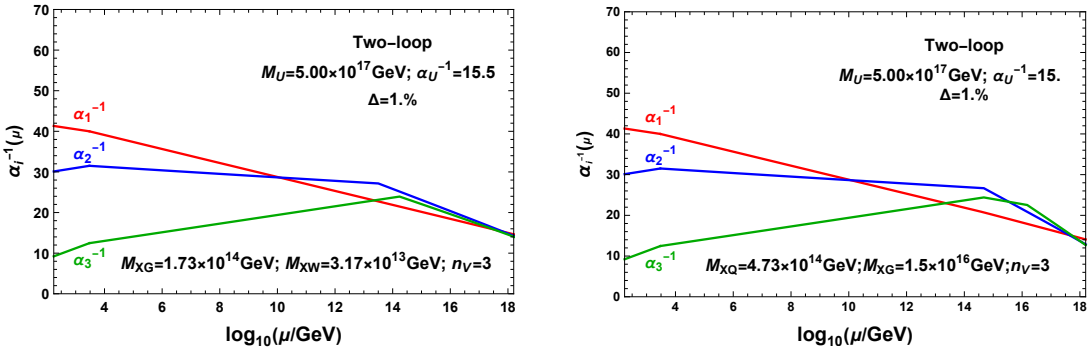

(a) (b)

Figure 13. Two-loop evolution of gauge couplings for the **Model 8** with vector-like particles. In the model, $k_Y = \frac{10}{7} \times \frac{5}{3}$ and $k_2 = 1$. The string-scale gauge coupling relations can be achieved by adding $3(XG + XW)$ (a) and $3(XQ + \overline{XQ}) + 3XG$ (b).

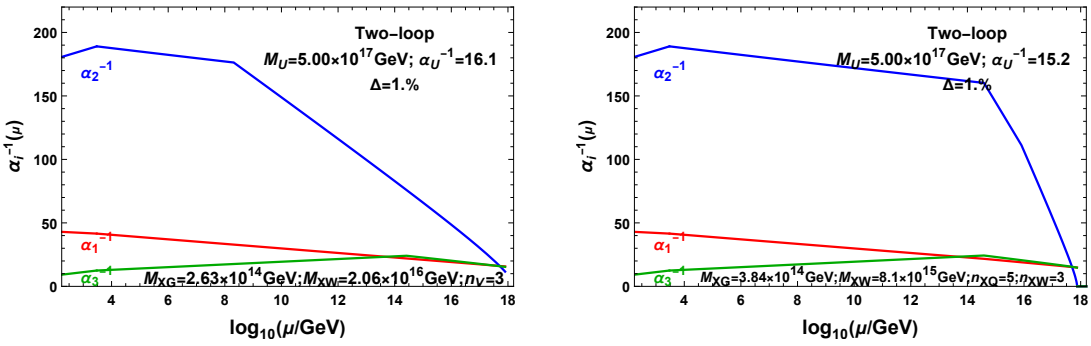

(a) (b)

Figure 14. Two-loop evolution of gauge couplings for the **Model 9** with vector-like particles. In the model, $k_Y = \frac{11}{8} \times \frac{5}{3}$ and $k_2 = \frac{1}{6}$. The string-scale gauge coupling relation can be achieved by adding $3(XG + XW)$ (a) and $5(XQ + \overline{XQ}) + 3XW$ (b).

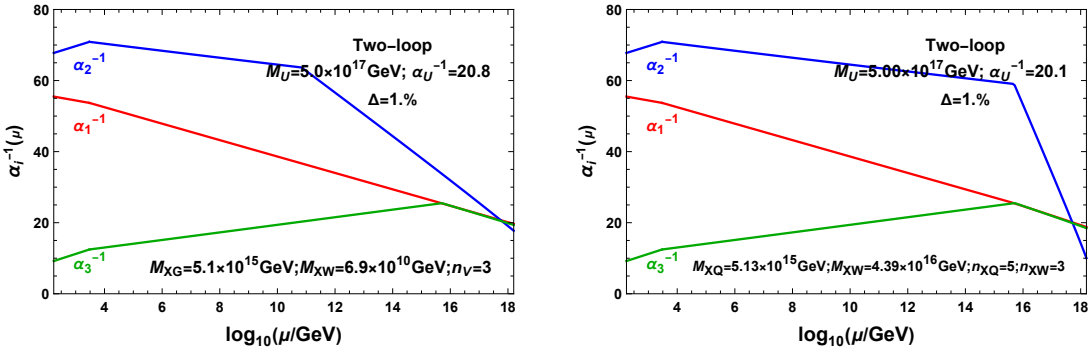

(a) (b)

Figure 15. Two-loop evolution of gauge couplings for the **Model 10** with vector-like particles. In the model, $k_Y = \frac{50}{47} \times \frac{5}{3}$ and $k_2 = \frac{4}{9}$. The string-scale gauge coupling relation can be achieved by adding $3(XG + XW)$ (a) and $5(XQ + \overline{XQ}) + 3XW$ (b).

JHEP03(2023)210

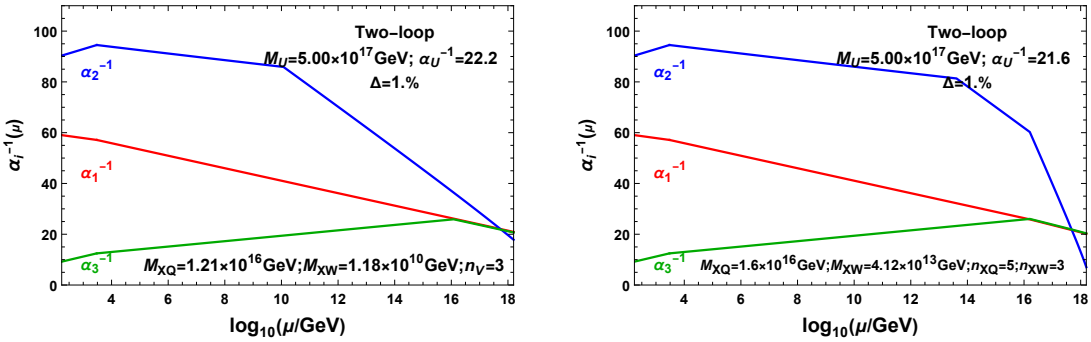

(a) (b)

Figure 16. Two-loop evolution of gauge couplings for the **Model 11** without and with vector-like particles. In the model, $k_Y = 1 \times \frac{5}{3}$ and $k_2 = \frac{1}{3}$. The string-scale gauge coupling relation can be achieved by adding $3(XG + XW)$ (a) and $5(XQ + \overline{XQ}) + 3XW$ (b).

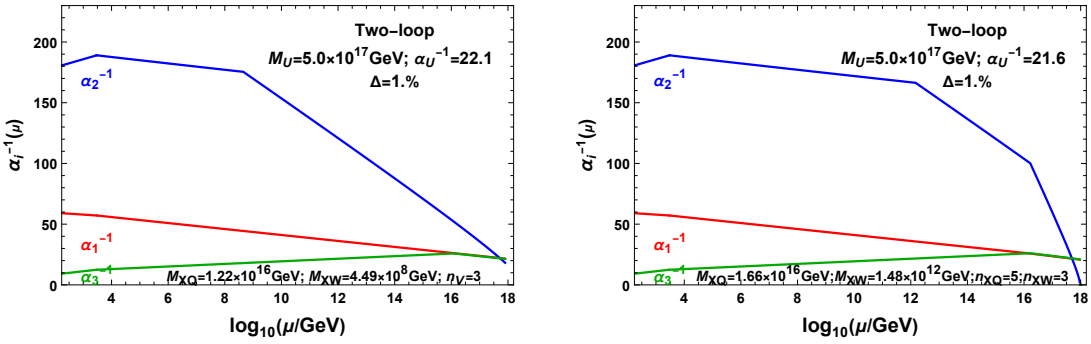

(a) (b)

Figure 17. Two-loop evolution of gauge couplings for the **Model 12** with vector-like particles. In the model, $k_Y = \frac{35}{32} \times \frac{5}{3}$ and $k_2 = \frac{1}{6}$. The string-scale gauge coupling relation can be achieved by adding $3(XG + XW)$ (a) and $5(XQ + \overline{XQ}) + 3XW$ (b).

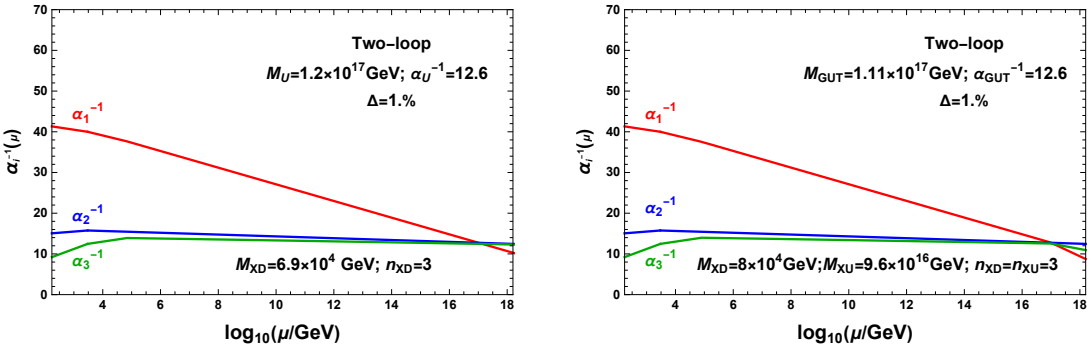

(a) (b)

Figure 18. Two-loop evolution of gauge couplings for the **Model 16** with vector-like particles. In this model, $k_Y = \frac{10}{7} \times \frac{5}{3}$ and $k_2 = 2$. The string-scale gauge coupling relation can be achieved by adding $3(XD + \overline{XD})$ (a) as well as $3(XU + \overline{XU})$ (b).

JHEP03(2023)210

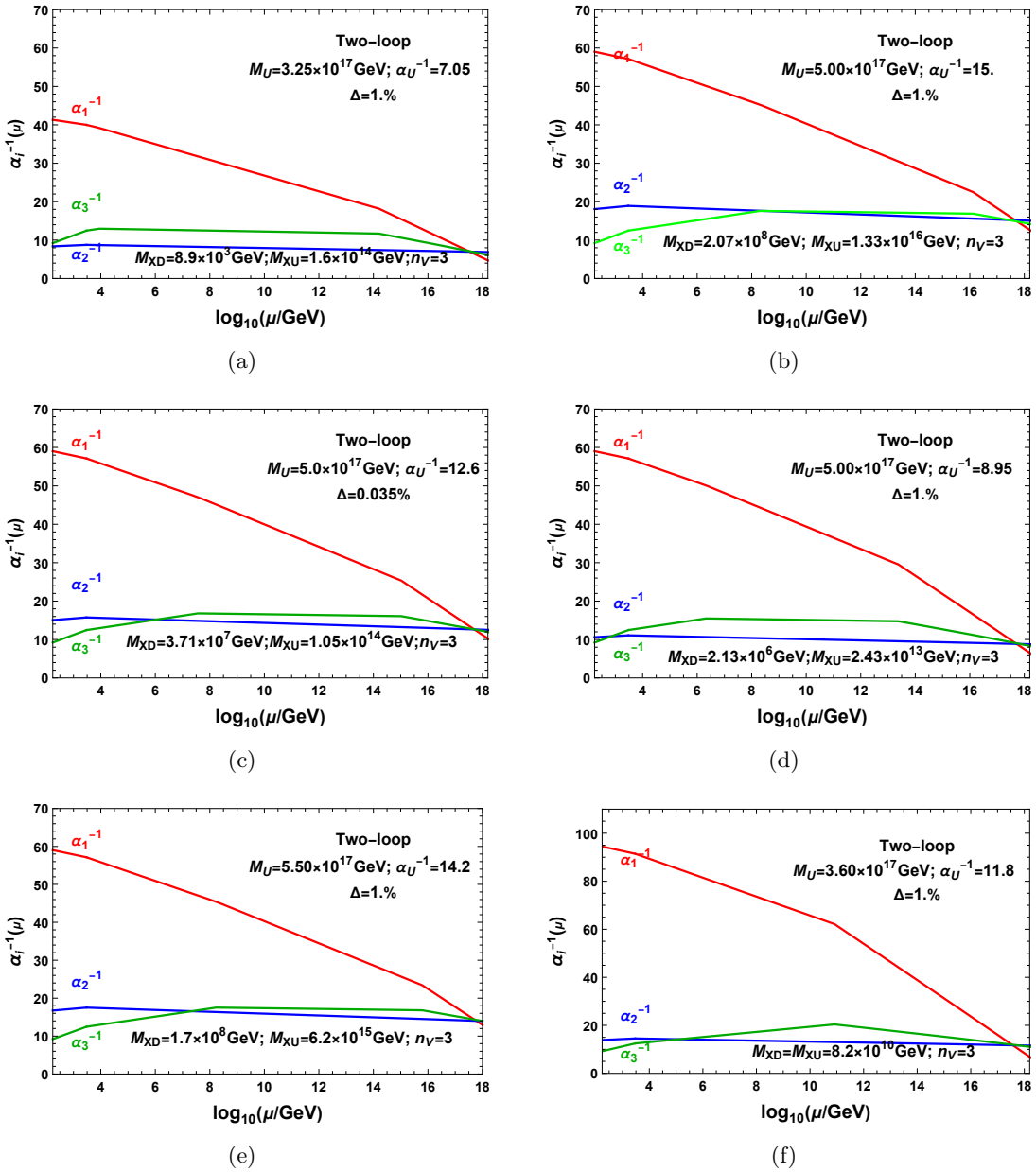

Figure 19. Two-loop evolution of gauge couplings for the **Model 18** (a), **Model 19** (b), **Model 20** (c), **Model 21** (d), **Model 22** (e) and **Model 23** (f) with vector-like particles. The string-scale gauge coupling relation can be achieved by adding $3(XD + \overline{XD}) + 3(XU + \overline{XU})$.

JHEP03(2023)210

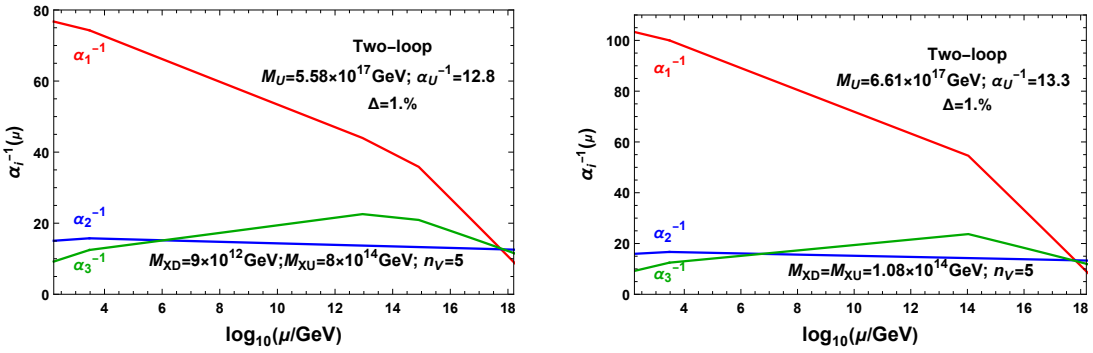

(a) (b)

Figure 20. Two-loop evolution of gauge couplings for the **Model 24** (a) and **Model 25** (b) with vector-like particles. In this model, $k_Y = \frac{10}{13} \times \frac{5}{3}$ and $k_2 = 2$. The string-scale gauge coupling relation can be achieved by adding $5(XD + \overline{XD}) + 5(XU + \overline{XU})$.

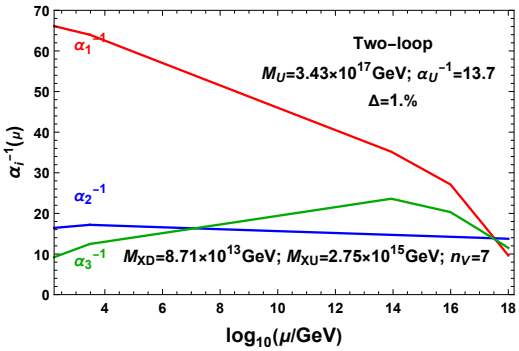

Figure 21. Two-loop evolution of gauge couplings for the **Model 26** with vector-like particles. In this model, $k_Y = \frac{25}{28} \times \frac{5}{3}$ and $k_2 = \frac{11}{6}$. The string-scale gauge coupling relation can be achieved by adding $7(XD + \overline{XD}) + 7(XU + \overline{XU})$.

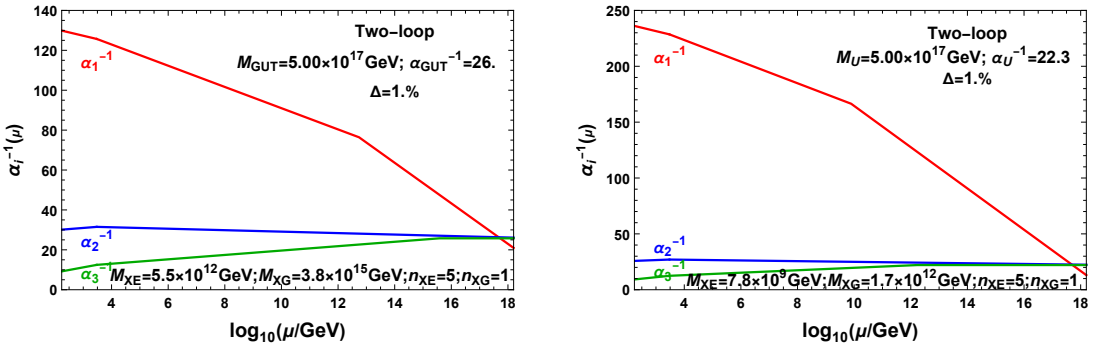

(a) (b)

Figure 22. Two-loop evolution of gauge couplings for the **Model 28** (a) and **Model29** (b) with vector-like particles. The string-scale gauge coupling relation can be achieved by adding $5(XE + \overline{XE}) + XG$.

JHEP03(2023)210

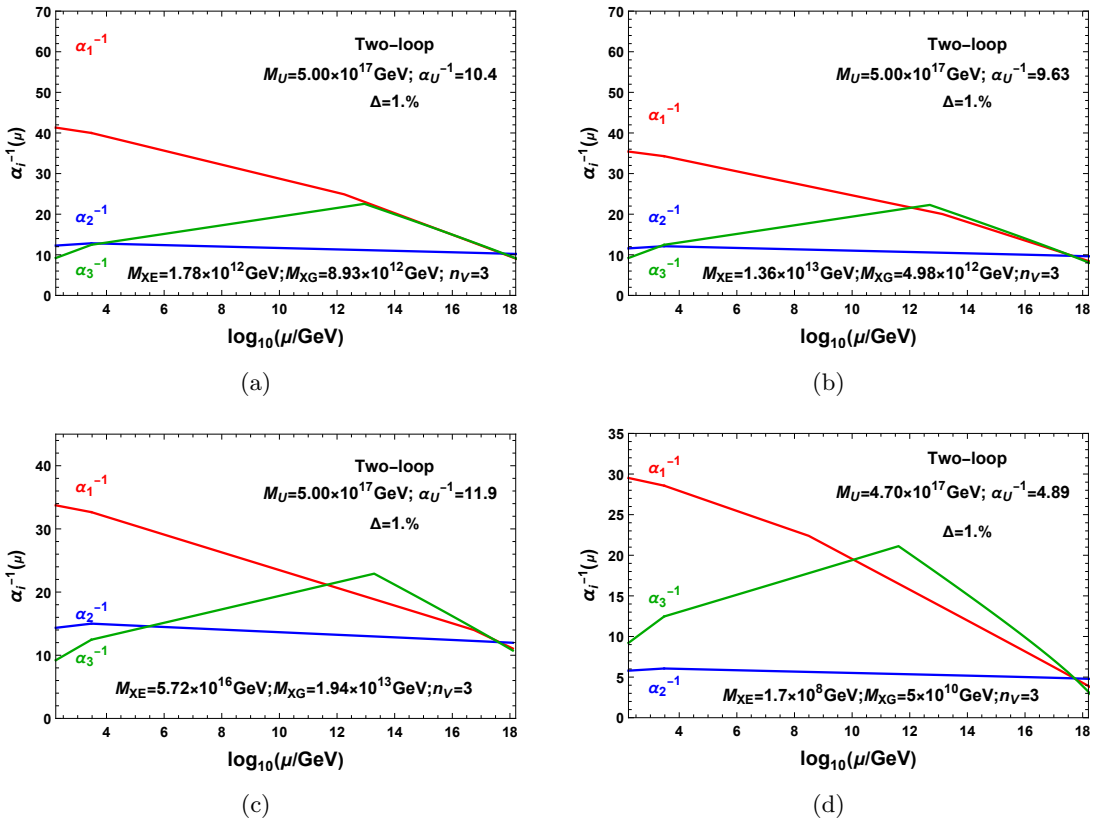

Figure 23. Two-loop evolution of gauge couplings for the **Model 30** (a), **Model 31** (b), **Model 32** (c) and **Model 33** (d) with vector-like particles. The string-scale gauge coupling relation can be achieved by adding $3(XE + \overline{XE}) + 3XG$.

JHEP03(2023)210

Open Access. This article is distributed under the terms of the Creative Commons Attribution License (CC-BY 4.0), which permits any use, distribution and reproduction in any medium, provided the original author(s) and source are credited. SCOAP^3 supports the goals of the International Year of Basic Sciences for Sustainable Development.

References

[1] J.D. Lykken, E. Poppitz and S.P. Trivedi, *Branes with GUTs and supersymmetry breaking*, *Nucl. Phys. B* **543** (1999) 105 [hep-th/9806080] [INSPIRE].

[2] M. Cvetic, M. Plumacher and J. Wang, *Three family type IIB orientifold string vacua with nonAbelian Wilson lines*, *JHEP* **04** (2000) 004 [hep-th/9911021] [INSPIRE].

[3] M. Cvetic, A.M. Uranga and J. Wang, *Discrete Wilson lines in $N = 1$ $D = 4$ type IIB orientifolds: A systematic exploration for Z_6 orientifold*, *Nucl. Phys. B* **595** (2001) 63 [hep-th/0010091] [INSPIRE].

[4] G. Aldazabal, L.E. Ibanez, F. Quevedo and A.M. Uranga, *D-branes at singularities: A bottom up approach to the string embedding of the standard model*, *JHEP* **08** (2000) 002 [hep-th/0005067] [INSPIRE].

[5] M. Berkooz, M.R. Douglas and R.G. Leigh, *Branes intersecting at angles*, *Nucl. Phys. B* **480** (1996) 265 [hep-th/9606139] [INSPIRE].

[6] M. Cvetic, T. Li and T. Liu, *Supersymmetric Pati-Salam models from intersecting D6-branes: A road to the standard model*, *Nucl. Phys. B* **698** (2004) 163 [hep-th/0403061] [INSPIRE].

[7] C.-M. Chen, T. Li, V.E. Mayes and D.V. Nanopoulos, *Variations of the hidden sector in a realistic intersecting brane model*, *J. Phys. G* **35** (2008) 095008 [arXiv:0704.1855] [INSPIRE].

[8] G. Aldazabal et al., *Intersecting brane worlds*, *JHEP* **02** (2001) 047 [hep-ph/0011132] [INSPIRE].

[9] M. Cvetic, G. Shiu and A.M. Uranga, *Three family supersymmetric standard-like models from intersecting brane worlds*, *Phys. Rev. Lett.* **87** (2001) 201801 [hep-th/0107143] [INSPIRE].

[10] R. Blumenhagen, L. Gorlich and T. Ott, *Supersymmetric intersecting branes on the Type IIA T^6/Z_4 orientifold*, *JHEP* **01** (2003) 021 [hep-th/0211059] [INSPIRE].

[11] C.-M. Chen et al., *A supersymmetric flipped* SU(5) *intersecting brane world*, *Phys. Lett. B* **611** (2005) 156 [hep-th/0501182] [INSPIRE].

[12] R. Blumenhagen, M. Cvetic, P. Langacker and G. Shiu, *Toward realistic intersecting D-brane models*, *Ann. Rev. Nucl. Part. Sci.* **55** (2005) 71 [hep-th/0502005] [INSPIRE].

[13] G. Aldazabal et al., *$D = 4$ chiral string compactifications from intersecting branes*, *J. Math. Phys.* **42** (2001) 3103 [hep-th/0011073] [INSPIRE].

[14] L.E. Ibanez, F. Marchesano and R. Rabadan, *Getting just the standard model at intersecting branes*, *JHEP* **11** (2001) 002 [hep-th/0105155] [INSPIRE].

[15] M. Sabir, T. Li, A. Mansha and X.-C. Wang, *The supersymmetry breaking soft terms, and fermion masses and mixings in the supersymmetric Pati-Salam model from intersecting D6-branes*, *JHEP* **04** (2022) 089 [arXiv:2202.07048] [INSPIRE].

[16] G. Honecker and J. Vanhoof, *Yukawa couplings and masses of non-chiral states for the Standard Model on D6-branes on T^6/Z_6'*, *JHEP* **04** (2012) 085 [arXiv:1201.3604] [INSPIRE].

JHEP03(2023)210

[17] G. Honecker, I. Koltermann and W. Staessens, *Deformations, Moduli Stabilisation and Gauge Couplings at One-Loop*, *JHEP* **04** (2017) 023 [arXiv:1702.08424] [INSPIRE].

[18] P. Anastasopoulos, *Orientifolds, anomalies and the standard model*, Ph.D. thesis, Crete University, Greece (2005) [hep-th/0503055] [INSPIRE].

[19] P. Anastasopoulos, T.P.T. Dijkstra, E. Kiritsis and A.N. Schellekens, *Orientifolds, hypercharge embeddings and the Standard Model*, *Nucl. Phys. B* **759** (2006) 83 [hep-th/0605226] [INSPIRE].

[20] P. Anastasopoulos, E. Kiritsis and A. Lionetto, *On mass hierarchies in orientifold vacua*, *JHEP* **08** (2009) 026 [arXiv:0905.3044] [INSPIRE].

[21] P. Anastasopoulos, G.K. Leontaris and N.D. Vlachos, *Phenomenological Analysis of D-Brane Pati-Salam Vacua*, *JHEP* **05** (2010) 011 [arXiv:1002.2937] [INSPIRE].

[22] P. Anastasopoulos, G.K. Leontaris, R. Richter and A.N. Schellekens, SU(5) *D-brane realizations, Yukawa couplings and proton stability*, *JHEP* **12** (2010) 011 [arXiv:1010.5188] [INSPIRE].

[23] P. Anastasopoulos, G.K. Leontaris, R. Richter and A.N. Schellekens, *Avoiding disastrous couplings in* SU(5) *orientifolds*, *Fortsch. Phys.* **59** (2011) 1144 [INSPIRE].

[24] J. Ecker, G. Honecker and W. Staessens, *D6-brane model building on* $\mathbb{Z}_2 \times \mathbb{Z}_6$*: MSSM-like and left-right symmetric models*, *Nucl. Phys. B* **901** (2015) 139 [arXiv:1509.00048] [INSPIRE].

[25] F. Marchesano, B. Schellekens and T. Weigand, *D-brane and F-theory Model Building*, arXiv:2212.07443 [INSPIRE].

[26] I. Antoniadis and S. Dimopoulos, *Splitting supersymmetry in string theory*, *Nucl. Phys. B* **715** (2005) 120 [hep-th/0411032] [INSPIRE].

[27] I. Antoniadis, *Aspects of string phenomenology*, *Int. J. Mod. Phys. A* **25** (2010) 4727 [INSPIRE].

[28] E. Kiritsis, *Orientifolds, and the search for the standard model in string theory*, *Les Houches* **87** (2008) 45 [INSPIRE].

[29] E. Kiritsis, *D-branes in standard model building, gravity and cosmology*, *Phys. Rept.* **421** (2005) 105 [hep-th/0310001] [INSPIRE].

[30] C.-M. Chen, T. Li, V.E. Mayes and D.V. Nanopoulos, *A realistic world from intersecting D6-branes*, *Phys. Lett. B* **665** (2008) 267 [hep-th/0703280] [INSPIRE].

[31] C.-M. Chen, T. Li, V.E. Mayes and D.V. Nanopoulos, *Towards realistic supersymmetric spectra and Yukawa textures from intersecting branes*, *Phys. Rev. D* **77** (2008) 125023 [arXiv:0711.0396] [INSPIRE].

[32] M. Cvetic and I. Papadimitriou, *More supersymmetric standard-like models from intersecting D6-branes on type IIA orientifolds*, *Phys. Rev. D* **67** (2003) 126006 [hep-th/0303197] [INSPIRE].

[33] M. Cvetic, I. Papadimitriou and G. Shiu, *Supersymmetric three family* SU(5) *grand unified models from type IIA orientifolds with intersecting D6-branes*, *Nucl. Phys. B* **659** (2003) 193 [hep-th/0212177] [INSPIRE].

[34] M. Cvetic, P. Langacker and G. Shiu, *Phenomenology of a three family standard like string model*, *Phys. Rev. D* **66** (2002) 066004 [hep-ph/0205252] [INSPIRE].

[35] M. Cvetic, P. Langacker and G. Shiu, *A three family standard-like orientifold model: Yukawa couplings and hierarchy*, *Nucl. Phys. B* **642** (2002) 139 [hep-th/0206115] [INSPIRE].

JHEP03(2023)210

[36] M. Cvetic, P. Langacker and J. Wang, *Dynamical supersymmetry breaking in standard-like models with intersecting D6-branes*, *Phys. Rev. D* **68** (2003) 046002 [hep-th/0303208] [INSPIRE].

[37] M. Cvetic and I. Papadimitriou, *Conformal field theory couplings for intersecting D-branes on orientifolds*, *Phys. Rev. D* **68** (2003) 046001 [*Erratum ibid.* **70** (2004) 029903] [hep-th/0303083] [INSPIRE].

[38] G. Honecker, *Chiral supersymmetric models on an orientifold of $Z_4 \times Z_2$ with intersecting D6-branes*, *Nucl. Phys. B* **666** (2003) 175 [hep-th/0303015] [INSPIRE].

[39] C.-M. Chen, T. Li and D.V. Nanopoulos, *Standard-like model building on Type II orientifolds*, *Nucl. Phys. B* **732** (2006) 224 [hep-th/0509059] [INSPIRE].

[40] M.R. Douglas and W. Taylor, *The landscape of intersecting brane models*, *JHEP* **01** (2007) 031 [hep-th/0606109] [INSPIRE].

[41] J. Halverson, B. Nelson and F. Ruehle, *Branes with Brains: Exploring String Vacua with Deep Reinforcement Learning*, *JHEP* **06** (2019) 003 [arXiv:1903.11616] [INSPIRE].

[42] G.J. Loges and G. Shiu, *Breeding Realistic D-Brane Models*, *Fortsch. Phys.* **70** (2022) 2200038 [arXiv:2112.08391] [INSPIRE].

[43] G.J. Loges and G. Shiu, *134 billion intersecting brane models*, *JHEP* **12** (2022) 097 [arXiv:2206.03506] [INSPIRE].

[44] M. Cvetic, P. Langacker, T.-J. Li and T. Liu, *D6-brane splitting on type IIA orientifolds*, *Nucl. Phys. B* **709** (2005) 241 [hep-th/0407178] [INSPIRE].

[45] M. Cvetic, G. Shiu and A.M. Uranga, *Chiral four-dimensional N=1 supersymmetric type 2A orientifolds from intersecting D6 branes*, *Nucl. Phys. B* **615** (2001) 3 [hep-th/0107166] [INSPIRE].

[46] T. Li, A. Mansha and R. Sun, *Revisiting the supersymmetric Pati-Salam models from intersecting D6-branes*, *Eur. Phys. J. C* **81** (2021) 82 [arXiv:1910.04530] [INSPIRE].

[47] T. Li et al., *$N = 1$ supersymmetric $\mathrm{SU}(12)_C \times \mathrm{SU}(2)_L \times \mathrm{SU}(2)_R$ models, $\mathrm{SU}(4)_C \times \mathrm{SU}(6)_L \times \mathrm{SU}(2)_R$ models, and $\mathrm{SU}(4)_C \times \mathrm{SU}(2)_L \times \mathrm{SU}(6)_R$ models from intersecting D6-branes*, *Phys. Rev. D* **104** (2021) 046018 [INSPIRE].

[48] T. Li, A. Mansha and R. Sun, *Generalized Supersymmetric Pati-Salam Models from Intersecting D6-branes*, arXiv:1912.11633 [INSPIRE].

[49] T. Li, R. Sun and C. Zhang, *Four-family supersymmetric Pati-Salam models from intersecting D6-branes*, *Commun. Theor. Phys.* **74** (2022) 065201 [arXiv:2202.10252] [INSPIRE].

[50] W. He, T. Li, R. Sun and L. Wu, *The final model building for the supersymmetric Pati-Salam models from intersecting D6-branes*, *Eur. Phys. J. C* **82** (2022) 710 [arXiv:2112.09630] [INSPIRE].

[51] W. He, T. Li and R. Sun, *The complete search for the supersymmetric Pati-Salam models from intersecting D6-branes*, *JHEP* **08** (2022) 044 [arXiv:2112.09632] [INSPIRE].

[52] J.R. Ellis, S. Kelley and D.V. Nanopoulos, *Probing the desert using gauge coupling unification*, *Phys. Lett. B* **260** (1991) 131 [INSPIRE].

[53] P. Langacker and M.-X. Luo, *Implications of precision electroweak experiments for M_t, ρ_0, $\sin^2\theta_W$ and grand unification*, *Phys. Rev. D* **44** (1991) 817 [INSPIRE].

JHEP03(2023)210

[54] U. Amaldi, W. de Boer and H. Furstenau, *Comparison of grand unified theories with electroweak and strong coupling constants measured at LEP*, *Phys. Lett. B* **260** (1991) 447 [INSPIRE].

[55] K.R. Dienes, *String theory and the path to unification: A review of recent developments*, *Phys. Rept.* **287** (1997) 447 [hep-th/9602045] [INSPIRE].

[56] I. Antoniadis, E. Kiritsis, J. Rizos and T.N. Tomaras, *D-branes and the standard model*, *Nucl. Phys. B* **660** (2003) 81 [hep-th/0210263] [INSPIRE].

[57] I. Antoniadis, M. Atkins and X. Calmet, *Brane World Models Need Low String Scale*, *JHEP* **11** (2011) 039 [arXiv:1109.1160] [INSPIRE].

[58] C. Bachas, C. Fabre and T. Yanagida, *Natural gauge coupling unification at the string scale*, *Phys. Lett. B* **370** (1996) 49 [hep-th/9510094] [INSPIRE].

[59] J.L. Lopez, D.V. Nanopoulos and A. Zichichi, *Supersymmetric photonic signals at LEP*, *Phys. Rev. Lett.* **77** (1996) 5168 [hep-ph/9609524] [INSPIRE].

[60] R. Blumenhagen, D. Lust and S. Stieberger, *Gauge unification in supersymmetric intersecting brane worlds*, *JHEP* **07** (2003) 036 [hep-th/0305146] [INSPIRE].

[61] V. Barger, J. Jiang, P. Langacker and T. Li, *Non-canonical gauge coupling unification in high-scale supersymmetry breaking*, *Nucl. Phys. B* **726** (2005) 149 [hep-ph/0504093] [INSPIRE].

[62] J. Jiang, T. Li and D.V. Nanopoulos, *Testable Flipped* $\mathrm{SU}(5) \times \mathrm{U}(1)_X$ *Models*, *Nucl. Phys. B* **772** (2007) 49 [hep-ph/0610054] [INSPIRE].

[63] V. Barger et al., *Implications of Canonical Gauge Coupling Unification in High-Scale Supersymmetry Breaking*, *Nucl. Phys. B* **793** (2008) 307 [hep-ph/0701136] [INSPIRE].

[64] J. Jiang, T. Li, D.V. Nanopoulos and D. Xie, *F*-SU(5), *Phys. Lett. B* **677** (2009) 322 [arXiv:0811.2807] [INSPIRE].

[65] J. Jiang, T. Li, D.V. Nanopoulos and D. Xie, *Flipped* $\mathrm{SU}(5) \times \mathrm{U}(1)_X$ *Models from F-Theory*, *Nucl. Phys. B* **830** (2010) 195 [arXiv:0905.3394] [INSPIRE].

[66] C. Kokorelis, *Gauge Unification from Split Supersymmetric String Models*, *PoS* **CORFU2015** (2016) 070 [arXiv:1610.01742] [INSPIRE].

[67] H.-Y. Chen et al., *The Minimal GUT with Inflaton and Dark Matter Unification*, *Eur. Phys. J. C* **78** (2018) 26 [arXiv:1703.07542] [INSPIRE].

[68] H.-Y. Chen et al., *Natural Higgs Inflation, Gauge Coupling Unification, and Neutrino Masses*, *Int. J. Mod. Phys. A* **35** (2020) 2050117 [arXiv:1805.00161] [INSPIRE].

[69] R. Blumenhagen, B. Kors and D. Lust, *Type I strings with F flux and B flux*, *JHEP* **02** (2001) 030 [hep-th/0012156] [INSPIRE].

[70] R. Blumenhagen, M. Cvetic and T. Weigand, *Spacetime instanton corrections in 4D string vacua: The seesaw mechanism for D-Brane models*, *Nucl. Phys. B* **771** (2007) 113 [hep-th/0609191] [INSPIRE].

[71] M. Haack et al., *Gaugino Condensates and D-terms from D7-branes*, *JHEP* **01** (2007) 078 [hep-th/0609211] [INSPIRE].

[72] B. Florea, S. Kachru, J. McGreevy and N. Saulina, *Stringy Instantons and Quiver Gauge Theories*, *JHEP* **05** (2007) 024 [hep-th/0610003] [INSPIRE].

JHEP03(2023)210

[73] V. Barger, C.-W. Chiang, J. Jiang and T. Li, *Axion models with high-scale supersymmetry breaking*, *Nucl. Phys. B* **705** (2005) 71 [hep-ph/0410252] [INSPIRE].

[74] I. Gogoladze, B. He and Q. Shafi, *New Fermions at the LHC and Mass of the Higgs Boson*, *Phys. Lett. B* **690** (2010) 495 [arXiv:1004.4217] [INSPIRE].

[75] M.E. Machacek and M.T. Vaughn, *Two Loop Renormalization Group Equations in a General Quantum Field Theory. 1. Wave Function Renormalization*, *Nucl. Phys. B* **222** (1983) 83 [INSPIRE].

[76] M.E. Machacek and M.T. Vaughn, *Two Loop Renormalization Group Equations in a General Quantum Field Theory. 2. Yukawa Couplings*, *Nucl. Phys. B* **236** (1984) 221 [INSPIRE].

[77] M.E. Machacek and M.T. Vaughn, *Two Loop Renormalization Group Equations in a General Quantum Field Theory. 3. Scalar Quartic Couplings*, *Nucl. Phys. B* **249** (1985) 70 [INSPIRE].

[78] G. Cvetic, C.S. Kim and S.S. Hwang, *Higgs mediated flavor changing neutral currents in the general framework with two Higgs doublets: An RGE analysis*, *Phys. Rev. D* **58** (1998) 116003 [hep-ph/9806282] [INSPIRE].

[79] V.D. Barger, M.S. Berger and P. Ohmann, *Supersymmetric grand unified theories: Two loop evolution of gauge and Yukawa couplings*, *Phys. Rev. D* **47** (1993) 1093 [hep-ph/9209232] [INSPIRE].

[80] V.D. Barger, M.S. Berger and P. Ohmann, *The supersymmetric particle spectrum*, *Phys. Rev. D* **49** (1994) 4908 [hep-ph/9311269] [INSPIRE].

[81] S.P. Martin and M.T. Vaughn, *Two loop renormalization group equations for soft supersymmetry breaking couplings*, *Phys. Rev. D* **50** (1994) 2282 [*Erratum ibid.* **78** (2008) 039903] [hep-ph/9311340] [INSPIRE].

[82] Particle Data Group collaboration, *Review of Particle Physics*, *Phys. Rev. D* **98** (2018) 030001 [INSPIRE].

[83] Particle Data Group collaboration, *Review of Particle Physics*, *PTEP* **2020** (2020) 083C01 [INSPIRE].

JHEP03(2023)210